

# A New Census of the variable star population in the Globular Cluster NGC 2419<sup>1</sup>

M. Di Criscienzo<sup>1</sup>, C. Greco<sup>2,3</sup>, V. Ripepi<sup>4</sup>, G. Clementini<sup>3</sup>, M. Dall’Ora<sup>4</sup>, M. Marconi<sup>4</sup>, I. Musella<sup>4</sup>, L. Federici<sup>3</sup>, L. Di Fabrizio<sup>5</sup>

<sup>1</sup>INAF- Osservatorio Astronomico di Roma, via Frascati, 33, Monte Porzio Catone, I-00040, Rome, Italy

<sup>2</sup>Observatoire de Geneve, 51, ch. Des Maillettes, CH-1290 Sauverny, Switzerland

<sup>3</sup>INAF- Osservatorio Astronomico di Bologna, via Ranzani 1, I-40127, Bologna Italy

<sup>4</sup>INAF- Osservatorio Astronomico di Capodimonte, via Moiarello 16, I-80131 Napoli, Italy

<sup>5</sup>INAF-Centro Galileo Galilei & Telescopio Nazionale Galileo, PO Box 565, 38700 S. Cruz de La Palma, Spain

## ABSTRACT

We present  $B, V$  and  $I$  CCD light curves for 101 variable stars belonging to the globular cluster NGC 2419, 60 of which are new discoveries, based on datasets obtained at the TNG, SUBARU and HST telescopes. The sample includes 75 RR Lyrae stars (of which 38 RRab, 36 RRc and one RRd), one Population II Cepheid, 12 SX Phoenicis variables, 2  $\delta$ Scuti stars, 3 binary systems, 5 long-period variables, and 3 variables of uncertain classification. The pulsation properties of the RR Lyrae variables are close to those of Oosterhoff type II clusters, consistent with the low metal abundance and the cluster horizontal branch morphology, disfavoring (but not totally ruling out) an extragalactic hypothesis for the origin of NGC 2419. The observed properties of RR Lyrae and SX Phoenicis stars are used to estimate the cluster reddening and distance, using a number of different methods. Our final value is  $\mu_0$  (NGC 2419) =  $19.71 \pm 0.08$  mag ( $D = 87.5 \pm 3.3$  kpc), with  $E(B - V) = 0.08 \pm 0.01$  mag,  $[\text{Fe}/\text{H}] = -2.1$  dex in the Zinn & West metallicity scale, and a value of  $M_V$  that sets  $\mu_0$  (LMC) = 18.52 mag. This value is in good agreement with most recent literature estimates of the distance to NGC 2419.

*Subject headings:* —Galaxy: halo —globular clusters: general —globular clusters: individual (NGC 2419) —stars: horizontal branch —stars: variables: other —techniques: photometry

## 1. Introduction

Galactic Globular Clusters (GGCs) offer a fundamental tool for both tracing the properties of our Galaxy in the present epoch, and for piecing together its formation history. They are old, massive, spread all over the Galaxy and generally bright, hence can be observed up to large Galactocentric distances ( $\simeq 100$  kpc) and through regions of high extinction. GGCs have long been used as

tools to understand how the Galactic halo formed. Two alternative scenarios have been suggested in the past: according to Eggen, Sandage & Lynden Bell (1962) the halo formed by the rapid dissipative collapse of a single massive protogalactic cloud, whereas Searle & Zinn (1978) suggested it was assembled over an extended time via infall and capture of smaller fragments. Currently, the most favourite scenario implies that the main body of the Milky Way (MW,  $R_{\text{gc}} < 10$  kpc) formed in a monolithic collapse, while the outer parts ( $R_{\text{gc}} > 15$  kpc) were assembled by capture of protogalactic fragments or at least experienced a number of

<sup>1</sup>Based on data collected at the 3.5 m Telescopio Nazionale Galileo, operated by INAF, and the SUBARU and Hubble Space Telescope archives

merging events (van den Bergh & Mackey 2004). According to this scenario a fraction of the “young halo” clusters is expected to have formed in external dwarf galaxies, and to have later accreted when the parent galaxies merged and were destroyed by the MW. Many signatures of past and present interactions have been found in the MW halo and a number of GGCs may have an extragalactic origin. This is the case of  $\omega$  Cen and M54. These clusters are both “peculiar” in some respects.  $\omega$  Cen hosts multiple stellar populations (see e.g. Bedin 2004; Rey et al. 2004; Sollima et al. 2005) and is suggested to be the stripped core of a disrupted dwarf galaxy (Villanova et al. 2007, and references therein). On the other hand, M54 is thought to belong to the Sagittarius (Sgr) dwarf spheroidal galaxy (dSph) that is currently merging with the MW (see e.g. Layden & Sarajedini 2000, Monaco et al. 2005, Bellazzini et al. 2008). There is another GC in the Milky Way for which an extragalactic origin was suggested: NGC2419, one of the most remote and luminous cluster in the MW. As  $\omega$  Cen and M54, NGC2419 is significantly looser than expected for its brightness in the  $M_V$  vs half-light radius ( $R_h$ ) plane (Mackey & van den Bergh 2005).

Apart from the similarity with  $\omega$  Cen and M54, other two pieces of evidence support the idea that NGC 2419 might have an extragalactic origin and be the remnant of a dwarf galaxy tidally disrupted by the MW (van den Bergh & Mackey 2004, Mackey & van den Bergh 2005):

1. NGC 2419 has a large core radius,  $r_c = 0.32'$  (Bellazzini 2007), corresponding to  $r_c \sim 8$  pc at its distance ( $\sim 90$  kpc, Ripepi et al. 2007), and the cluster half-light radius ( $r_h = 0.96'$ , Bellazzini 2007), corresponding to  $r_h \sim 23$  pc, is much larger than that of GCs of similar luminosity, and about as large as the largest nuclei of dwarf elliptical galaxies (Mackey & van den Bergh 2005);
2. Newberg et al. (2003) find that NGC 2419 appears to lie within an overdensity of A-type stars connected to the tidal tails of the Sagittarius dSph, and suggest that the cluster might once be associated to this galaxy.

NGC 2419 has a central velocity dispersion ( $\sigma_0=4.14\pm 0.48$  km/s<sup>-1</sup>, Baumgardt 2009) lower

than that of other dSphs for which this quantity was measured. According to this value in the  $L_V$  vs  $\sigma_0$  plane (Faber & Jackson 1976), the cluster lies  $3\sigma$  below the “fundamental plane” relations for Galactic GCs (see de Grijs et al. 2005). NGC 2419 has other unusual properties as a globular cluster NGC 2419 has unusual properties also as a globular cluster.

Its Galactocentric distance ( $d = 90$  kpc) is typical of an outer halo cluster, however the cluster is definitely metal poorer ( $[Fe/H] = -2.10$  dex, Zinn & West 1984, Suntzeff et al. 1988,  $[Fe/H] = -2.20 \pm 0.009$  dex, Carretta et al. 2009) than other outer halo clusters and belongs to the most metal-poor group of MW GCs most of which (with the only exception of AM-4) are located within  $R_{GC} \simeq 20$  Kpc. NGC 2419 is also one of the five most luminous GCs in the MW ( $M_V = -9.58$  mag, Harris 1996,  $-9.4$  mag, Bellazzini 2007; Baumgardt 2009) breaking the rule that GCs in the outer halo (and those at  $R_{GC} \geq 50$  in particular) are, on average, fainter than GCs in the inner halo (van den Bergh & Mackey 2004). In conclusion, NGC 2419 appears to be peculiar both in terms of being a GC (either Galactic or external) and as the possible remnant of a disrupted dwarf galaxy.

After the pioneering photographic study of Racine & Harris (1975) who published a first color-magnitude-diagram (CMD) of the cluster deep to  $V = 22.2$  mag, NGC 2419 has been the subject of many photometric studies both from the ground and with the Hubble Space Telescope (HST). CMDs for the cluster were published by Christian & Heasley (1988), Harris et al. (1997), Stetson (1998, 2005); Saha et al. (2005), Sirianni et al. (2005), and, more recently, by Bellazzini (2007), Ripepi et al. (2007), Dalessandro et al. (2008), and Sandquist & Hess (2008). Due to the large distance, the ground-based CMDs of NGC 2419 do not generally go fainter than the cluster main sequence turn-off (TO). On the other hand, the HST-based CMDs, while deeper, (Harris et al. 1997’s in particular, which reaches  $V \sim 27.8$  mag), cover only small portions of the cluster and, also, generally lack stars brighter than  $V \sim 18-19$  mag, since often they are saturated in the HST images.

In Ripepi et al. (2007) we published a CMD of

NGC 2419 which, for the first time, is both deep and covers a very large field of view around the cluster. Our CMD samples a total range of about 9 magnitudes, from the tip of the cluster red giant branch (RGB) around  $V \sim 17$  mag, down to  $V \sim 25.7$  mag, about 2.3 mag below the TO, and extends over an area encompassing more than 1 tidal radius ( $r_t = 8.74'$ , Trager, King & Djorgovski 1995) in the North-South direction and about 2 tidal radii in East-West from the cluster center (see Fig.1). Ripepi et al. (2007) CMD shows that the horizontal branch (HB) of NGC 2419 extends down to an extremely long blue tail ending with the “blue hook” for  $V \geq 23.8$  mag (see Brown et al. 2010, for a detailed discussion of the blue hook origin in NGC2419 and other GGCs). The cluster also has a prominent Blue Straggler Star (BSS) sequence populated by an extraordinary large number of BSSs (see also Dalessandro et al. 2008).

As anticipated in Ripepi et al. (2007), we have performed a new extensive study of the cluster variable stars and detected 60 new variables, among which 39 are RR Lyrae stars that double the cluster RR Lyrae population, and 12 are SX Phoenicis (SX Phe) variables located in the BSS region of the CMD. The only previous study of the NGC 2419 variables is by Pinto & Rosino (1977, hereafter PR) and is based on photographic plates and “by eye” photometry. PR identified 41 variables mainly located in the outer parts of the cluster, of which 32 were recognized as RR Lyrae stars. In this paper we present a full description of the database we employed in Ripepi et al. (2007), describe in detail the study and properties of the variable stars and publish the catalogue of light curves. Observations and data reduction techniques used to process the total time-series of NGC 2419 are described in Section 2. In Section 3 we detail the methods used to detect and study the variable stars, and present the complete catalog of light curves. In Section 4 we describe the analysis of the various types of variables (RR Lyrae, SX Phe, long period and miscellaneous variables) and their distribution on the cluster CMD. In Section 5 we discuss the cluster distance based on its RR Lyrae and SX Phe stars. In particular, we compare the observed properties of the RR Lyrae stars with the predictions of nonlinear pulsation models to constrain the cluster distance modulus.

Finally, in Section 6 we provide a summary of our results.

## 2. Observations and data reduction

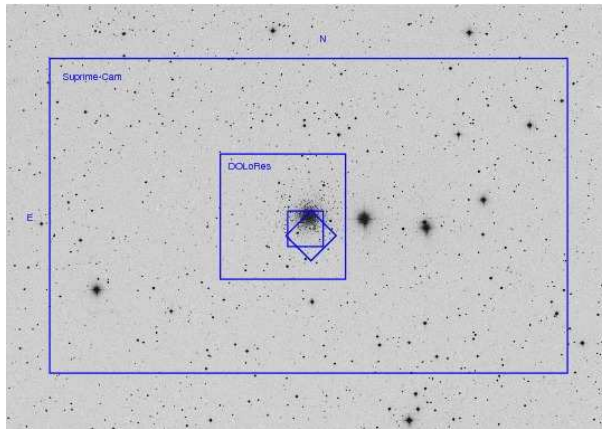


Fig. 1.— Total field of view covered by our data for NGC 2419. Boxes mark the fields covered by each of the 3 different imagers we used in our study: Suprime-CAM at the SUBARU telescope (largest box), DOLORES at the TNG, and WFPC2 on board the HST (smallest boxes).

Time-series  $B, V$  photometric observations of NGC 2419 (RA=07h38m24.0s, decl=38°454'00", J2000) were obtained between 2003 September and 2004 February with DOLORES at the 3.5m TNG telescope<sup>2</sup>. Observations were performed in service mode under the requirement of seeing better than 1.5 arcsec. The TNG data were complemented by F555W and F814W Wide Field Planetary Camera 2 (WFPC2) on board of the HST<sup>3</sup> archival observations of the cluster spanning 6 years from 1994, May to 2000, March (Programs ID 5481, 7628, 7630, 8095), and by  $V, I$  photometry obtained with the Suprime-Cam of the SUBARU 8.2 m telescope<sup>4</sup> along four nights in 2002, December. Typical exposure times of the HST observations range from 40s to 1400s in F555W, and from 40s to 1300s in F814W. The SUBARU data consist instead of 30s and 180s exposures in both the  $I$  and  $V$  bands. The total

<sup>2</sup><http://www.tng.iac.es/instruments/lrs/>

<sup>3</sup><http://www.stsci.edu/hst/wfpc2>

<sup>4</sup><http://www.subarutelescope.org/Observing/Instruments/SCam/index.html>

time-series dataset comprises 20  $B$ , 212  $V$  and 65  $I$  images. Logs of the observations and details of the instrumental set-up at the various telescopes are provided in Table 1. The large field of view of the Suprime-Cam ( $34 \times 27$  arcmin<sup>2</sup>), covered by a mosaic of 10 CCDs, and dithering of the telescope pointings resulted in the survey of a total area of  $50 \times 43$  arcmin<sup>2</sup> centered on NGC 2419, which includes both the TNG and HST fields. Results presented in this paper cover a region extending  $\pm 10.5'$  in North-South and  $\pm 18.3'$  in East-West from the cluster center. The area, which corresponds to five partially overlapping CCDs of the SUBARU mosaic, is shown in Fig. 1.

Images were pre-reduced following standard techniques (bias subtraction and flat-field correction) with IRAF<sup>5</sup>. We then performed PSF photometry of the pre-processed images running the DAOPHOTII/ALLSTAR/ALLFRAME packages (Stetson 1987, 1992) on the TNG, HST and SUBARU datasets, separately. Typical internal errors of the  $V$  band photometry per single phase point at the level of the HB are in the range from 0.01 to 0.15 mag. We checked for consistency the photometry by randomly extracting several pairs of images and computing the differences of the magnitudes of the stars in common to each pair, which showed a scatter consistent with the intrinsic photometric error, with no trend with magnitude and position of the stars along the frames.

The absolute photometric calibration was obtained by using local standards in NGC 2419 from P.B. Stetson's list<sup>6</sup>. A total of about 400 standard stars covering approximately the color intervals  $-0.2 < (B - V) < 1.8$  mag and  $-0.2 < (V - I) < 2.0$  mag were used to derive a set of linear calibration equations for  $B$ ,  $V$  and  $I$ , respectively:

$$\begin{aligned} B &= b_{TNG} + (0.017 \pm 0.003) \times (b_{TNG} - v_{SUB}) + \\ &\quad + (7.709 \pm 0.0003) \\ V &= v_{SUB} + (6.123 \pm 0.014) \\ I &= i_{SUB} + (0.039 \pm 0.002) \times (v_{SUB} - i_{SUB}) + \end{aligned}$$

<sup>5</sup>IRAF is distributed by the National Optical Astronomical Observatories, which are operated by the Association of Universities for Research in Astronomy, Inc., under cooperative agreement with the National Science Foundation

<sup>6</sup>Available at <http://cadwww.dao.nrc.ca/standards/>

$$+(5.811 \pm 0.002)$$

Zero point uncertainties are of 0.022, 0.014 and 0.014 mag in  $B$ ,  $V$  and  $I$ , respectively.

The  $V$ ,  $V - I$  CMD of NGC 2419 based on the SUBARU dataset was published and discussed in Ripepi et al. (2007). Here we focus on the cluster variable stars.

### 3. Identification of the variable stars

Candidate variable stars were first identified on the  $V$  frames of NGC 2419 obtained with the TNG by using the Optimal Image Subtraction technique as performed within the package ISIS 2.1 (Alard 1999, 2000). We identified about 300 candidate variables over the field of view covered by the TNG observations, a large fraction of them were found towards the cluster centre. To increase the number of phase points and obtain a better definition of periods and light curves, the TNG candidate variables were then counteridentified on the HST and SUBARU catalogs. Moreover, since the SUBARU observations better resolve the cluster inner regions and, at the same time, cover a larger external area compared to the TNG, an independent search for variables was carried out on the SUBARU  $V$ -band dataset by applying the following procedure: i) we calculated the Fourier transform (in the Schwarzenberg-Czerny 1996 formulation) of each star of the SUBARU photometric catalogue for which we had at least 25 epochs; ii) we averaged this transform to estimate the noise; 3) we calculated the signal-to-noise ratio dividing by the noise the peak with maximum amplitude in the transform. We then checked all the stars with high S/N, that for the RR Lyrae stars typically means S/N in the range from 6.5 to 100. All candidate variables identified by any of the two independent techniques described above were then checked for variability using GRaTiS (Graphic Analyzer of Time Series), a custom software developed at the Bologna Observatory by P. Montegriffo (see Di Fabrizio 1999; Clementini et al. 2000), which allows a period search using both the Lomb periodogram (Lomb 1976, Scargle 1982) and the best fit of the data with a truncated Fourier series (Barning 1963). We confirmed the variability of 101 stars, and derived period and classification in type for 98 of them. Whenever applicable, the study of the light curves was performed by com-

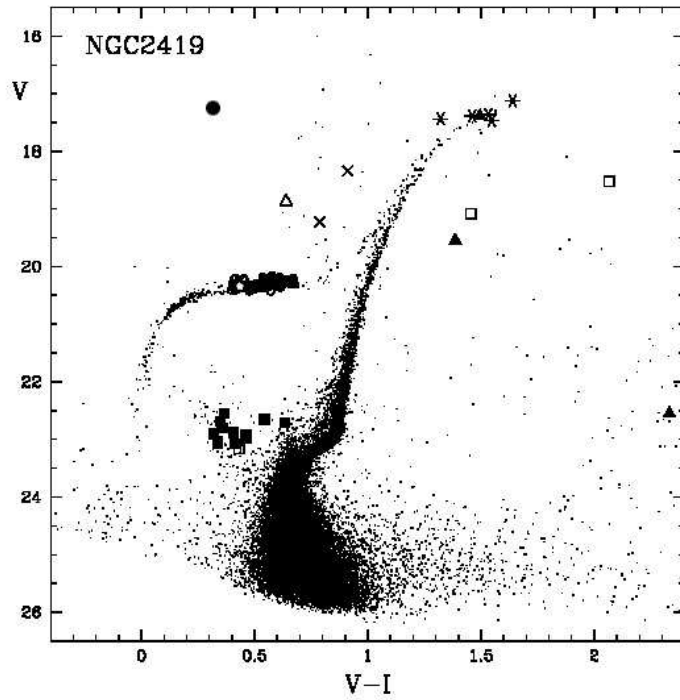


Fig. 2.—  $V$  vs  $V - I$  CMD of NGC 2419 from the SUBARU dataset, with the cluster variables plotted according to their intensity-averaged magnitudes and colors, and using different symbols for the various type of variables. Filled circles:  $ab$ -type RR Lyrae stars (RRab); open circles: first overtone (RRc) RR Lyrae; pentagon: double-mode (RRd) star; open triangle: Population II Cepheid; filled squares: SX Phoenicis stars; open squares: binary systems; asterisks: long period and semiregular variables; crosses:  $\delta$  Scuti stars; filled triangles: variable stars with non reliable classification in type (NC).

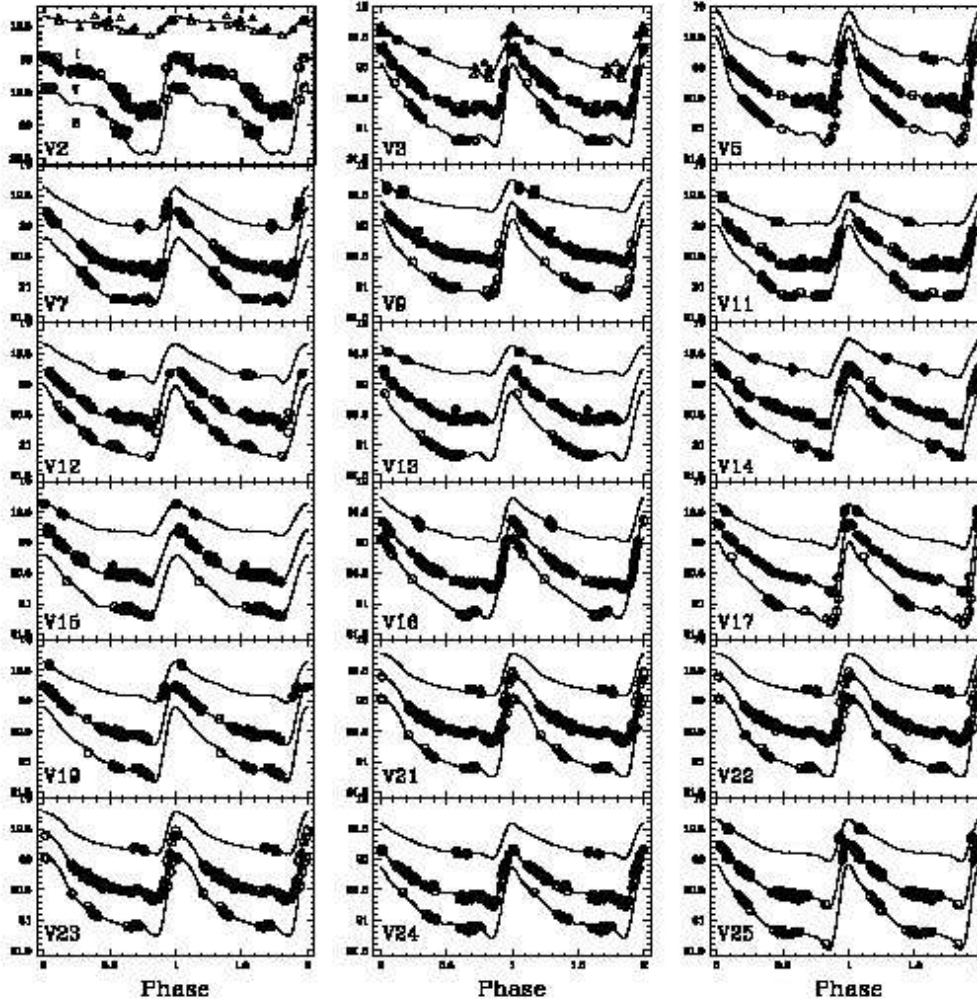


Fig. 3.—  $B, V, I$  light curves of fundamental-mode RR Lyrae stars in NGC 2419. Open and filled symbols are used for the TNG and SUBARU data, respectively. Open triangles are the HST data. Lines are models obtained by properly scaling the star's  $V$  light curve according to the procedure described in Section 3. The full catalogue of RRab light curves (38 stars) is published in the electronic edition of the paper. The errors on each phase point are of the same order of magnitude of the photometric accuracy reported in Table 1 for each telescope.

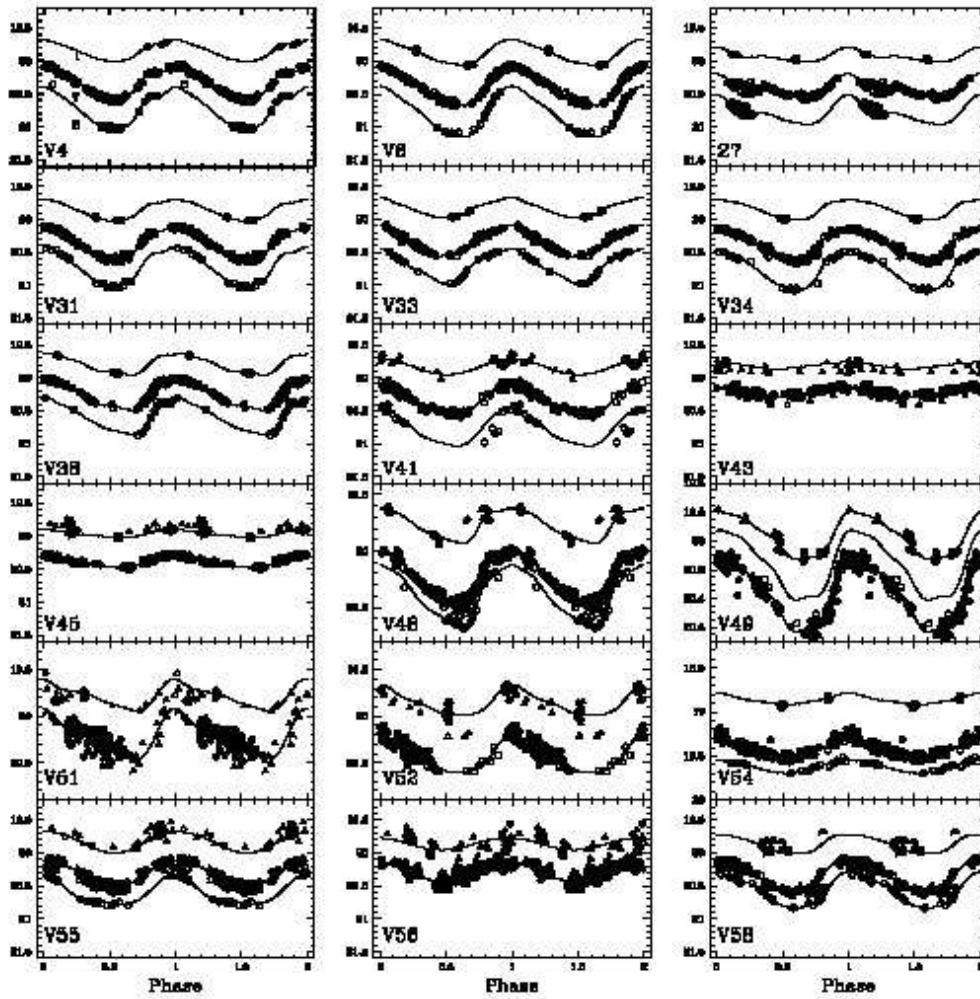


Fig. 4.— Same as Fig. 3 but for first-overtone RR Lyrae stars. The full catalogue of RRc light curves (36 stars) is published in the electronic edition of the paper.

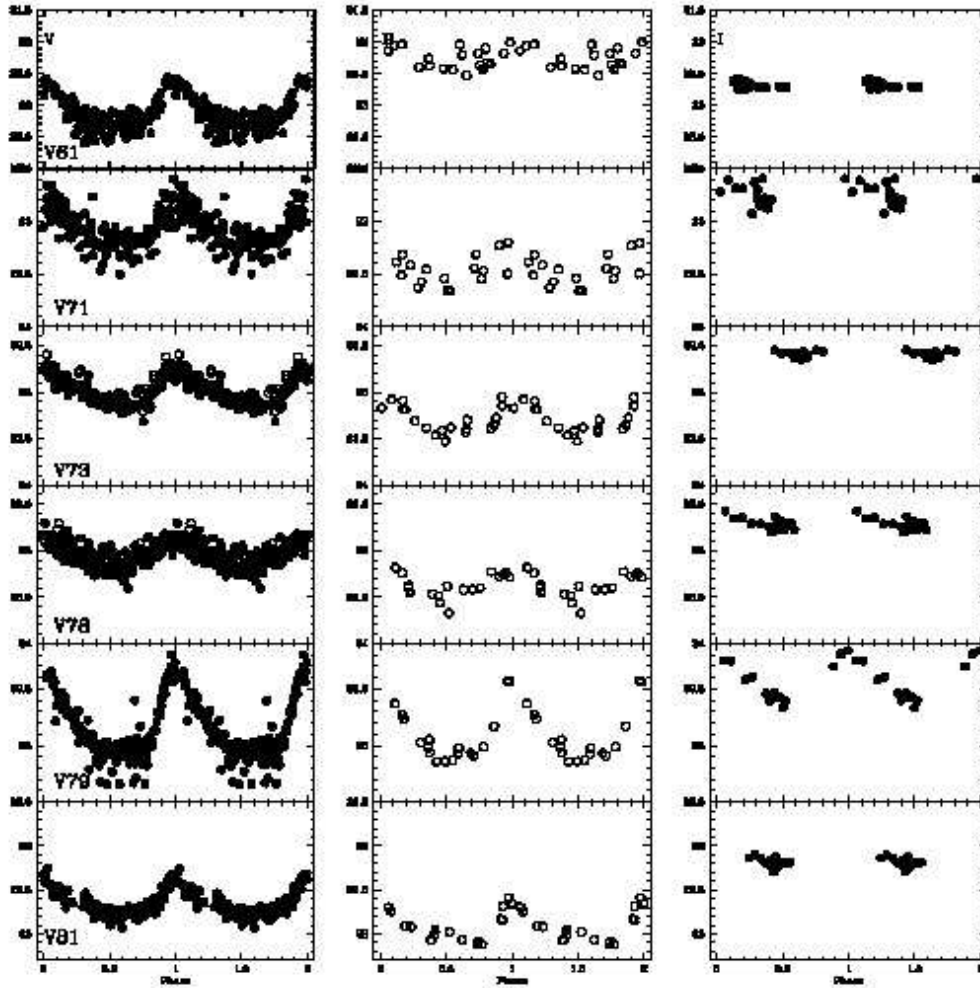


Fig. 5.—  $B, V, I$  light curves of SX Phoenicis stars. Symbols are as in Fig. 3. The full catalogue of SX Phe light curves (12 objects) is published in the electronic edition of the paper.

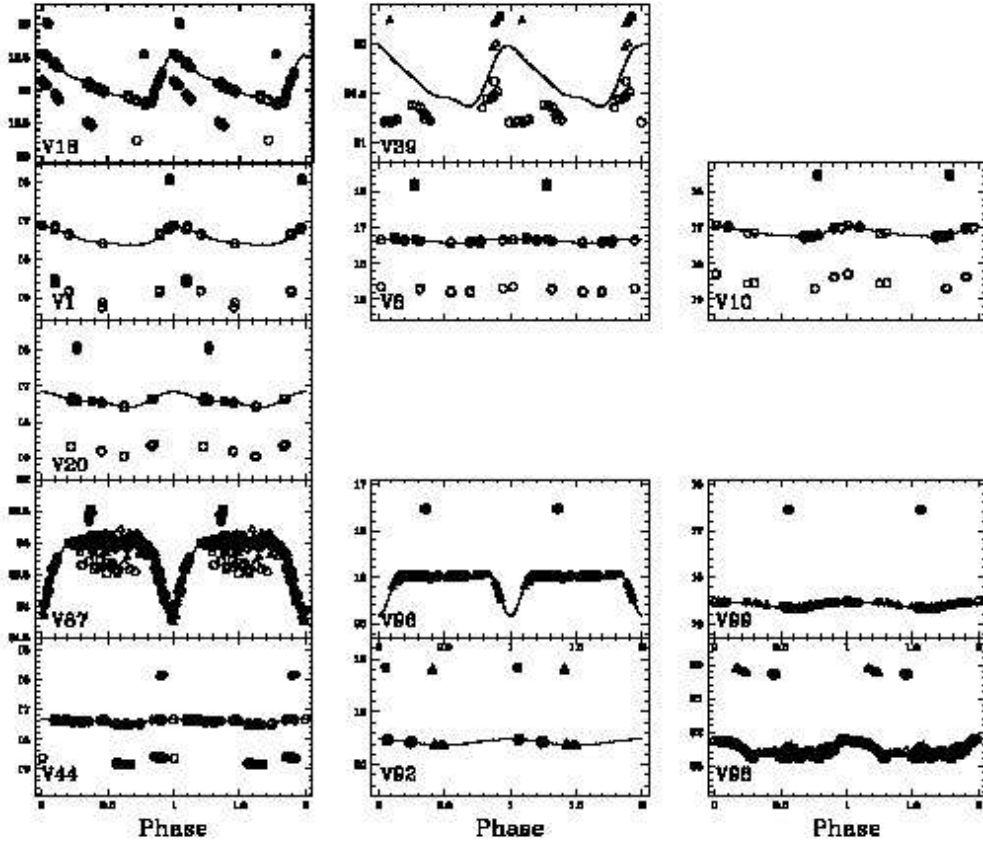


Fig. 6.—  $B, V, I$  light curves of Pop. II Cepheids (V18), RRd (V39), LPVs (V1, V8, V10, V20 and V86), binary systems (V87, V96 and V99), non classified variables (V44, V92 and V98), and  $\delta$ Scuti stars (V95 and V100). Symbols are as in Fig. 3.

binning data from the three different photometric catalogs (TNG, HST, SUBARU). To combine the photometry we selected a number of reference stars common to the three datasets, and studied the light curves using the differential photometry with respect to the comparison stars. The total number of phase points of the combined datasets ranges from 17 to 20, from 22 to 212, and from 2 to 65 in the  $B$ ,  $V$  and  $I$  bands, respectively, with optimal sampling of the  $V$  light curves of the RR Lyrae stars, acceptable coverage in  $B$ , and rather poor sampling in  $I$ , since the  $I$ -band observations are rather closely spaced in time. Periods were first derived from the  $V$ -band data alone, given the better sampling, then applied to the  $B$  and  $I$ -band data and iteratively improved. The large time baseline (ten years) covered by the combined dataset, allowed us to solve alias ambiguities which were rather severe when considering only individual datasets. The merged datasets also returned a better estimate of the period, epoch of maximum light and amplitudes of the light variation of the confirmed variable stars. Precision of the final period determinations is of 4-5 decimal places for variables with periods shorter than 2 days (95 objects) and increases up to 6 digits for stars with the three datasets available.

Our sample of variable stars in NGC 2419 includes 76 RR Lyrae stars, 1 Population II Cepheid, 12 SX Phe stars, 2  $\delta$  Scuti variables, 3 binaries, 5 long period variables (LPVs) near the cluster RGB tip, and 3 stars which we were not able to classify in type.  $V, B, I$  time-series photometry for each of the confirmed variables is provided in Table 2 (the full table is available from the authors upon request). Fig. 2 shows the  $V$  vs  $V - I$  CMD of NGC 2419 obtained from the SUBARU dataset, with the variable stars identified in our study plotted according to their intensity-averaged magnitudes and colors, and using different symbols for the various type of variables.

Identification and coordinates of the variable stars are provided in Table 3, along with type, period, time of maximum light, intensity-averaged  $\langle V \rangle$ ,  $\langle B \rangle$  and  $\langle I \rangle$  magnitudes, and amplitudes of the light variation ( $A_V$ ,  $A_B$  and  $A_I$ ). For the double-mode star (V39), in the table we list the period corresponding to the first-overtone pulsation. Notes on individual stars are provided in Section 3.1.

Variables from V1 to V41 were already known from PR study, while stars from V42 to V101 are new discoveries identified in the present work. We assigned to the latter identification numbers increasing with increasing the distance to the cluster center. The complete atlas of light curves is presented in Figs. 3 and 4 for fundamental-mode and first overtone RR Lyrae stars separately, in Fig. 5 for the SX Phe stars, and in Fig. 6, for the other types of variables (namely Population II Cepheids, LPVs, binaries, non classified and  $\delta$  Scuti variables).

The good sampling of the  $V$ -band light curves allowed us to obtain good best-fits of the visual data and a reliable estimate of the average  $V$  magnitude of the variable stars. On the other hand, given the small number of  $B$  and  $I$  phase points and the uneven distribution of the  $I$ -band observations, average  $B$  and  $I$  magnitudes are available only for a subsample of objects and are, in general, more uncertain than the  $V$  mean magnitudes. To recover the average magnitudes in  $B$  and  $I$  of the RR Lyrae stars, and thus be able to plot them on the cluster CMD, when the  $B$  and  $I$  data sampling was too sparse we used the star's  $V$  band light curve as a template and properly scaled it in amplitude to fit the  $B$  and  $I$  light curves. To constrain the scaling factors we computed  $A(B)/A(V)$ ,  $A(V)/A(I)$  ratios using literature  $B, V, I$  light curves of 130 RR Lyrae stars with good light curve parameters selected from the GCs M68, NGC 5466, NGC 5053, M3, NGC 6362, NGC 6229, NGC 3201, M5, IC 4499 (see Clement catalogue available at <http://www.astro.utoronto.ca/~cclement/> for references on individual clusters)<sup>7</sup>. The derived ratios, computed as weighted averages, are  $A(B)/A(V) = 1.29 \pm 0.02$ , and  $A(V)/A(I) = 1.58 \pm 0.03$  independently of the cluster metallicity and variable's pulsation mode.

Direct check of our scaling procedure and a fine tuning of the adopted amplitude ratios was possible for the  $B$  light curves because the  $\sim 20$  epochs available for this filter are evenly distributed and allowed us to directly fit the observed  $B$  light

<sup>7</sup>The sample includes both *ab*- and *c*-type RR Lyrae variables and we verified that the derived ratio values are independent of type. The  $A(B)/A(V)$  value is also in good agreement with the value defined for M15 (Corwin et al. 2008), whereas for  $A(V)/A(I)$  we neglected a very small trend with amplitude present in some clusters for the RRab stars.

curves of the vast majority of the RR Lyrae stars with very low errors ( $< 0.01$  mag) adopting an  $A(B)/A(V)$  ratio varying in the range from about 1.25 to 1.30. No direct check was possible instead of the adopted  $A(I)/A(V)$  ratio since the  $I$ -band light curves are, in general, too poorly sampled, with all data points clustered around two separate epochs. Thus, for this band we relied entirely upon the scaling value derived from the literature data. Additional checks showed that, varying the  $A(V)/A(I)$  ratio by 10%, translates into an error of about 3% in  $\langle I \rangle$ . Given the formal error of the  $A(V)/A(I)$  values ( $\sim 2\%$ ), we are thus confident that our procedure provides accurate mean  $I$  magnitudes, in spite of the uneven sampling of the light curves in this band. Indeed, once plotted on the cluster  $V, V - I$  CMD by using the  $\langle V - I \rangle$  colors derived with the above procedure the RR Lyrae stars appear to fall very well into the instability strip thus giving support to the reliability of our procedure. The  $A(V)/A(I)$  ratio derived for the RR Lyrae stars was also used to scale the light curves of the other types of pulsating variables, since pulsation is caused basically by the same physical mechanism in all pulsating variables. For the binary systems we adopted instead a ratio  $A(V)/A(I) = 1$  since variability in these stars is due to a geometrical effect, hence is acromatic.

As a final note, due to the worse seeing conditions and the coarse pixel scale of the TNG data with respect to the SUBARU images, the  $B$  light curves of several RR Lyrae stars are contaminated by companions and often have unreliable  $\langle B - V \rangle$  colors. For this reason we decided to plot the variable stars on the  $V, V - I$  (SUBARU dataset) CMD of NGC 2419 (Fig. 2).

### 3.1. Notes on individual stars

**V1, V8, V10, V20, V86:** these stars located around the cluster RGB tip are classified LPVs. They are saturated in all the HST frames and in the SUBARU 180s long exposures. Only the TNG and SUBARU frames with  $t_{exp}=30$ s were used to derive their light curves and pulsation properties. **V2:** this RRab is about one magnitude brighter than the HB, and being at the center of the cluster it is likely contaminated by companion stars which also may cause the bumpy light curves from 0.2 to 0.6 in phase.

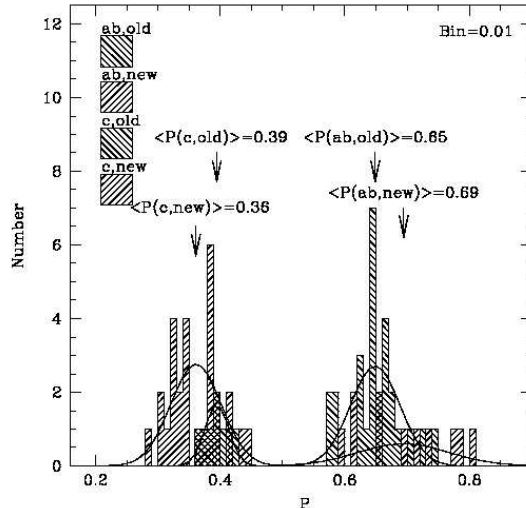


Fig. 7.— Period distribution of  $ab$ - and  $c$ - type RR Lyrae stars, divided into known ( $ab$ - $c$ , old) and newly discovered variables ( $ab$ - $c$ , new). Periods are in days.

**V27:** data from the TNG set are very scattered. The Fourier analysis gives several aliases which makes it difficult to define the period. The star was also observed by Baade (1935). The three sets of data (this paper, Baade, and PR) are not phased by the same period, probably because the period changed from  $P=0.35184$  days by Baade, to  $P=0.34896$  days by PR, to the value  $P=0.34519$  days inferred from our data.

**V37:** there is a shift in magnitude between SUBARU and TNG light curves, we used both datasets to define the period, but only the SUBARU data to derive mean magnitudes and amplitudes.

**V39:** double-mode RR Lyrae star with period ratio  $P_1/P_0=0.745$ . In Table 3 we report the pulsation characteristics of the first-overtone (FO) pulsation, the pulsation characteristics of the fundamental mode are  $P_F=0.54621$  d,  $A_V=0.347$ mag,  $A_B=0.454$ mag,  $A_I=0.305$ mag.

**V44:** this star is very bright and is saturated in the HST frames and in the SUBARU 180 s exposures, only the TNG images and the SUBARU frames with  $t_{exp}=30$  s could be used to derive its pulsation properties. The star has  $P \sim 0.9$  days

and rather small amplitudes. According to the position on the CMD V44 falls in the region of LPVs.

**V45:** the star is very close to the cluster center. The SUBARU data provide a  $V$  amplitude larger than the TNG data. In Table 3 we have reported the visual amplitude inferred from the SUBARU data, the amplitude of the TNG data is  $A_V > 0.416$ mag.

**V46:** the star is in the central part of the cluster and likely contaminated by other stars. We have used only the SUBARU data because less scattered than the TNG observations.

**V54:** the star, classified as first overtone RR Lyrae, has small amplitudes likely because contaminated by two companion stars.

**V62:** The star is contaminated by a very luminous source. The SUBARU data are not usable and the TNG data are very scattered.

**V70:** there is a shift in magnitude between TNG and SUBARU datasets for the star. In the present analysis we used only the TNG data which produce a smoother light curve.

**V65, V71, V79, V76:** these stars are in the central part of the cluster. There are systematic shifts among TNG, SUBARU and HST datasets of the four stars likely due to crowding and blending effects. All three datasets were used to estimate the periods, but only the SUBARU data to derive average magnitudes and amplitudes.

**V80:** the star is near a very bright source. Only the TNG dataset was used since produced smoother light curves.

**V83:** the star is in the blue straggler region and is tentatively classified as SX Phoenicis variable, however with its period of about 0.14 days significantly deviates from the SX Phe PL relation (see Fig. 13).

**V87:** binary system. In Table 3 we list the most probable period inferred for the star by the Lomb periodogram since it gives less scatter than the period inferred from the Fourier analysis ( $P=0.184716$  days,  $A_V=1.199$  mag,  $A_B=0.166$  mag, and  $A_V > 0.265$  mag).

**V89:** the star has very small amplitudes for a  $c$ -type RR Lyrae. It lies very close to the edge of the frames and this may partially explain the anomalous amplitudes.

#### 4. Properties of the NGC 2419 variable stars

In their study of the NGC 2419 variable stars PR identified 32 RR Lyrae stars, 1 Population II Cepheid, 4 red irregular/semiregular variables, and further 4 variables on the HB, likely RR Lyrae stars, for which they were not able to provide period and mode classification. Clement & Nemec (1990) later found that V39, which PR classify as a first overtone RR Lyrae star, is in fact a *double-mode* pulsator (RRd). In our study, we recovered and derived reliable periods for all the variables previously known in NGC 2419 by PR study, and detected 60 new variables that are mainly located in the cluster central regions. In the following we discuss the properties of the various types of variables, separately.

##### 4.1. The RR Lyrae stars

PR classified as fundamental mode RR Lyrae stars (RRab) 25 of the variables detected in NGC 2419 and further seven as first-overtone pulsators (RRc). According to the average periods  $\langle P_{ab} \rangle = 0.654$  days and  $\langle P_c \rangle = 0.384$  days they concluded that the cluster is an Oosterhoff type II (OoII) system (Oosterhoff 1939). This is consistent with the cluster low metal abundance and HB morphology, and strengthens the similarity with other three metal poor Galactic GCs, namely, M92, M15 and M68, which are also OoII systems. We will come back to this point later in this section. In our study we confirmed period and classification in types of the RR Lyrae stars found by PR. Our analysis also confirmed both periods and period ratio:  $P_1/P_0 = 0.745$  found for the double-mode RR Lyrae star (V39) by Clement & Nemec (1990). We also derived period and classification in type for the 4 variables for which PR do not provide an estimate of period, namely, V30, V38, V40, and V41. We find that two are *ab*-type and two are *c*-type RR Lyrae stars. As for the new discoveries they include 11 fundamental mode and 28 first overtone pulsators. The number of new *c*-type RR Lyrae stars discovered in the present study is remarkably high, and increases by a factor 5 the statistics of the RRc stars detected in NGC 2419 by PR. On the other hand, the new RRab stars extend the period range of the known fundamental-mode pulsators

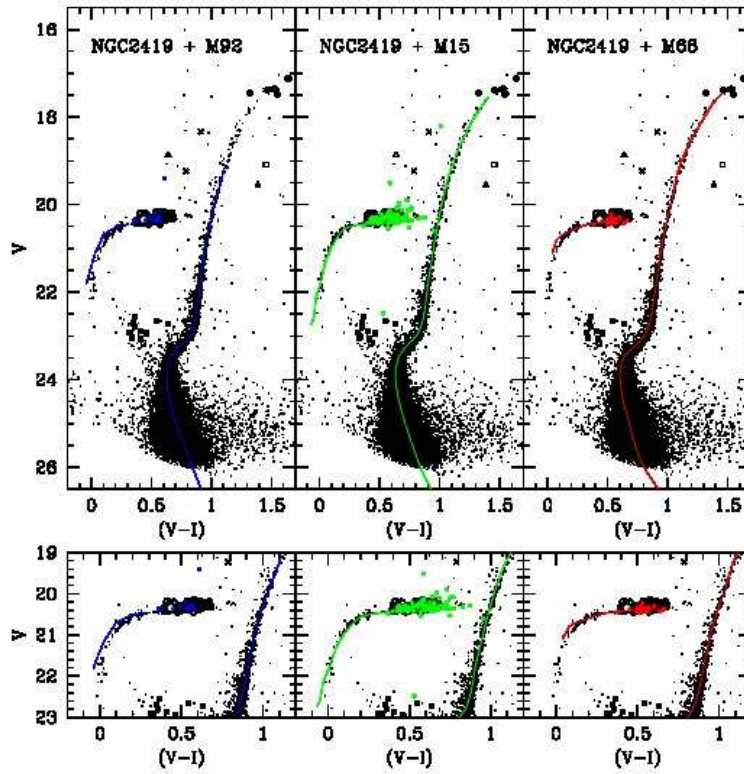


Fig. 8.— Comparison of CMD, HB morphology and distribution of the RR Lyrae stars on the HB of NGC 2419 with the mean ridge lines and RR Lyrae distribution of three metal poor, OoII, Galactic GCs, namely, M92 (left panels), M15 (central panels), and M68 (right panels). Symbols are the same as in Fig. 2.

in NGC2419 to longer periods, hence smaller amplitudes, than in PR. Most of the new RRc as well as the new RRab stars with longer periods were missed by PR because their small amplitudes and the location often towards the cluster center made them rather difficult to detect with traditional techniques. Summarizing, with the addition of the new variables the number of RR Lyrae stars in NGC 2419 becomes: 38 RRab, 36 RRc and 1 RRd star, and the ratio of number of RRc over number of RRc+RRab stars changes from 0.28 by PR to 0.49, in much better agreement with expectations for an Oo II cluster. The distributions in period of known and newly discovered RR Lyrae stars, are compared in Fig. 7 for *ab*- and *c*-type variables, separately, and clearly show that PR missed the variable stars with smaller amplitudes. The average period of the total sample of RR Lyrae stars is:  $\langle P_{ab} \rangle = 0.662$  d ( $\sigma = 0.055$ , average on 38 stars), and  $\langle P_c \rangle = 0.366$  d, ( $\sigma = 0.038$ , average on 36 stars), for fundamental-mode and first-overtone pulsators, respectively. The new values confirm and strengthen the classification of NGC 2419 as an OoII cluster. The minimum period of the RRab stars,  $P_{ab_{min}} = 0.576$  d, is in perfect agreement with values of prototypes OoII clusters like M15 (Corwin et al. 2008) and M68 Walker (1994). In Fig. 8 we compare the HB morphology and the distribution of the RR Lyrae stars on the NGC 2419 HB with the mean ridge lines and RR Lyrae distribution of three other metal poor, OoII, Galactic GCs, namely, M92 (left panels), M15 (central panels), and M68 (right panels of Fig. 8). The ridge lines for the three clusters were derived respectively from, Johnson & Bolte (1992); Rosenberg et al. (2000); Walker (1998), while mean magnitudes and colors for the RR Lyrae stars are from the studies of Kopacki (2001); Corwin et al. (2008); Walker (1998). Ridge lines and RR Lyrae stars of M92 were shifted by  $\Delta V = 5.25$  mag and  $\Delta(V - I) = 0.07$  mag, those of M15 by  $\Delta V = 4.55$  mag and  $\Delta(V - I) = -0.005$  mag, and those of M68 by  $\Delta V = 4.75$  mag and  $\Delta(V - I) = 0.04$  mag, in order to match NGC 2419. This comparison confirms the similarity of NGC 2419 to these three clusters. In particular, the ridge lines and HB morphology of M15 perfectly matches the CMD and HB of NGC 2419. Moreover, the shift required to match NGC 2419 allows us to get hints

on the reddening affecting NGC 2419. Indeed, adopting  $E(B - V) = 1.26E(V - I)$ , and the reddening reported by Harris (1996):  $E(B - V)_{M92} = 0.02 \pm 0.01$  mag,  $E(B - V)_{M15} = 0.10 \pm 0.01$  mag, and  $E(B - V)_{M68} = 0.05 \pm 0.01$  mag, we obtain  $E(B - V)_{NGC\ 2419} = 0.08 \pm 0.01$  mag. We note that this estimate is intermediate between the value obtained by Harris (1996) ( $E(B - V) = 0.11 \pm 0.01$  mag) from the average of a number of different sources and the value derived by Schlegel et al. (1998) ( $E(B - V) = 0.065 \pm 0.010$  mag). Finally, we note that the RR Lyrae instability strip (IS) of NGC 2419 is sharply defined and very well sampled by the cluster variables. Its boundaries are found at  $\langle V \rangle - \langle I \rangle = 0.40 \pm 0.01$  mag (blue edge), and  $\langle V \rangle - \langle I \rangle = 0.67 \pm 0.01$  mag (red edge).

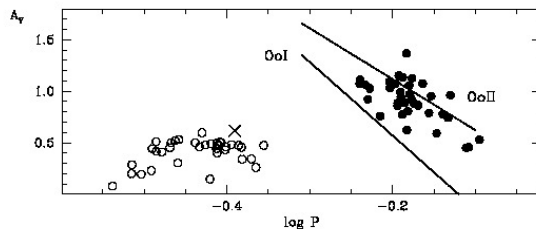


Fig. 9.— *V*-band period-amplitude diagram for RR Lyrae stars in NGC 2419. Filled and open circles are *ab*- and *c*-type RR Lyrae stars, respectively. The cross is the double-mode star. The two lines are the positions of the OoI and OoII GGCs according to Clement & Rowe (2000).

The *V*-band period-amplitude distribution (Bailey diagram) of the NGC 2419 RR Lyrae stars is shown in Fig. 9 and compared with the loci of OoI and OoII GGCs taken from Clement & Rowe (2000). The bulk of RRab stars clearly lies in the region defined by typical OoII GGCs, confirming the classification of NGC 2419 as OoII. The distribution of RRc stars shows a bell-shaped feature, as expected for a low metallicity RR Lyrae population (Di Criscienzo et al. 2004). A few RRab variables are scattered in the intermediate region between OoI and OoII types. The small ampli-

tudes of some of these variables located towards the cluster center may be due to contamination by companion stars as in the case of V42 and V80 which both also have very scattered light curves. The other stars which do not show any particular spatial distribution could either represent the short-period tail of the OoII period distribution, or could as well be undetected Blazhko variables (Blazhko (1907)).

In conclusion, according to our more complete census of the RR Lyrae population, NGC 2419 confirms its nature of a *pure* OoII globular cluster.

#### 4.2. The SX Phoenicis stars

As recently pointed out by Dalessandro et al. (2008) NGC 2419 contains one of the largest BSS population ever observed in a globular cluster, with more than 230 objects found in the brightest part of the main-sequence. Among them we detected 1 binary system, and 12 pulsating variables with periods in the range from 0.041 to 0.140d and hints, in some cases, for the existence of several secondary periodicities. They are likely SX Phoenicis stars. Light curves for the SX Phe stars are shown in Fig. 5. Since these stars obey a period luminosity (P-L) relation can be used as distance indicator to estimate the cluster distance. This is presented in Section 6 where we also discuss the mode classification of these 12 variables.

#### 4.3. Others types of variable stars

In Fig. 6 we show the light curves of other variable stars in our sample, namely one Population II Cepheid (V18), the double pulsator (V39), 5 long period variables (LPVs) near the tip of the cluster RGB (V1, V8, V10, V20 and V86), 3 binary systems (V87, V96 and V99). We also plot the light curves of 3 stars which we were not able to classify in type, as well as those of V95 and V100 which we classify as field  $\delta$  Scuti stars, since they have the typical period of this class of variables but are too bright to belong to NGC 2419.

## 5. Distance to NGC 2419 from the cluster RR Lyrae stars

In this section we calculate the distance to NGC 2419 using a number of methods based on the RR Lyrae stars.

### 5.1. $M_V$ -[Fe/H] relation

The RR Lyrae stars are primary distance indicators for Population II systems, since their absolute magnitude is almost constant and weakly dependent on metallicity. The average  $V$  apparent magnitude of the RR Lyrae stars can be used to derive an accurate estimate of the distance to NGC 2419, provided that the cluster metallicity and reddening are known, and that a value is adopted for the absolute magnitude of the RR Lyrae stars.

According to our study NGC 2419 contains 75 RR Lyrae stars. Their mean  $V$  magnitude is  $\langle V(\text{RR}) \rangle = 20.31 \pm 0.01$  mag ( $\sigma=0.06$ , average on 67 stars) excluding 8 objects which are either contaminated by companions or have incomplete light curves (namely, stars V2, V70, V57, V54, V65, V80, V58, V32). This average value defines very sharply the horizontal portion of the cluster HB. The metal abundance of NGC 2419 was estimated by Suntzeff et al. (1988) to be  $[\text{Fe}/\text{H}] = -2.1$  dex (on the Zinn & West metallicity scale) using low resolution spectra. This value is in agreement with the metal abundance derived for the cluster by Carretta et al. (2009) in their newly defined metallicity scale. Assuming for the absolute luminosity of the RR Lyrae stars at  $[\text{Fe}/\text{H}] = -1.5$ ,  $M_V = 0.54$  mag, which is consistent with a distance modulus for the Large Magellanic Cloud of  $18.52 \pm 0.09$  mag (Clementini et al. 2003),  $\Delta M_V / [Fe/H] = 0.214 (\pm 0.047)$  mag/dex (Gratton et al. 2004) for the slope of the RR Lyrae luminosity metallicity relation,  $E(B - V) = 0.08 \pm 0.01$  mag, and  $[\text{Fe}/\text{H}] = -2.1$  dex, the distance modulus of NGC 2419 derived from the mean luminosity of its RR Lyrae stars is  $(m-M)_0 = 19.65 \pm 0.09$  mag ( $D = 85.1 \pm 3.5$  kpc). The final errors on the distance include the standard deviation of the mean HB magnitude and the uncertainties in the photometry, reddening, and RR Lyrae absolute magnitude. The present value is in good agreement with literature values (Harris 1996) for the distance to NGC 2419 and is about 0.05 mag

longer than derived by Ripepi et al. (2007), due to the adoption of a different value for the absolute magnitude of the RR Lyrae stars.

## 5.2. Pulsation distances

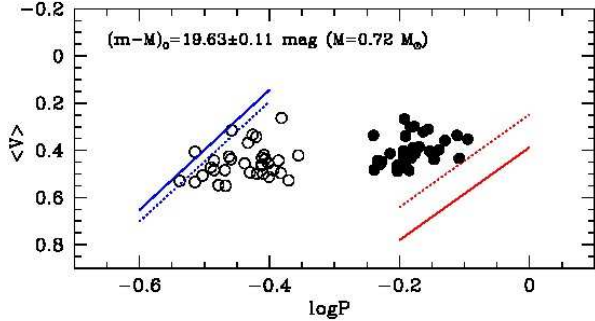


Fig. 10.— RR Lyrae stars of NGC 2419 in the  $M_V$  vs  $\log P$  plane. Filled and open circles are RRab and RRc pulsators, respectively. Solid and dashed lines are the theoretical boundaries of the instability strip calculated for values of the mixing length parameter of  $l/H_p=1.5$  and  $l/H_p=2.0$ , respectively.

We have estimated the distance to NGC 2419 with further four methods: i) the comparison of theoretical and empirical RR Lyrae first overtone blue edges (FOBE) and fundamental red edges (FRE) in the  $M_V$  versus  $\log P$  plane (Caputo 1997; Caputo et al. 2000; Di Criscienzo et al. 2004); ii) the theoretical Wesenheit function (Di Criscienzo et al. 2004); iii) the Period-Magnitude in the  $I$  band by Catelan et al. (2004); and iv) the light curve model fitting method (Bono et al. 2000). In order to compare the observed properties of RR Lyrae stars with the model predictions, we need an estimate of the mean mass of the pulsators. To this aim we can use the results of synthetic HB models as a function of HB type and global metallicity  $Z$  (see Di Criscienzo et al. 2004), hence, we have to convert the observed iron abundance ( $[Fe/H]=-2.1$  dex) into global metallicity  $Z$ . This transformation can be tricky due to the uncertainty of the  $\alpha$  enhancement for NGC 2419, for which there are no direct measurements available. Taking into account the to-

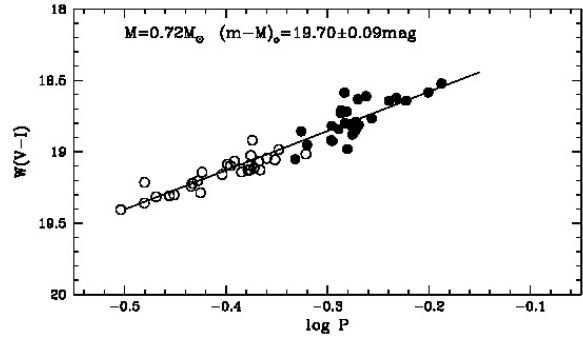


Fig. 11.— Comparison between observed and predicted Period-Wesenheit relation (symbols are as in Fig. 10). Periods of c-type pulsators were fundamentalized by adding the value  $+0.127$  to the logarithm of the star period (Di Criscienzo et al. 2004). The solid line represents the predicted fundamental-mode relation for  $M=0.72 M_\odot$ .

tal range of  $\alpha$  enhancement spanned by GGCs:  $\alpha=0$  and  $\alpha=0.5$  (Gratton et al. 2004), we obtain a range of  $Z=0.00015 \div 0.00035$  for the total metal abundance. We have then re-evaluated the cluster HB type ( $HB_{Lee-Zinn}$ ) based on our CMD of NGC 2419. This is the so-called Lee-Zinn parameter used to classify the morphology of the HB and depends on the number of stars inside and on either sides of the RR Lyrae IS ( $HB_{Lee-Zinn}=(B - R)/(B + V + R)$ ). We have derived its value using the SUBARU data and considering only RR Lyrae stars outside an area of 50 arcsec in radius from the cluster center (40 RR Lyrae stars in total). We took off the cluster center to alleviate problems related to blending and incompleteness. We obtain an HB type equal to 0.80 if we exclude the blue hook stars from the number  $B$  of stars bluer than the blue edge of the IS, 0.83 if we include also the blue hook stars, and 0.75 if only consider blue stars with  $V$  brighter than  $V=21$  mag. In the end we chose to use the value 0.80 for the HB type. It should be noted that at the metal abundance of NGC 2419 the HB type does not affect significantly the choice of the value for the mass (see Fig. 8 of Di Criscienzo et al. 2004). Using the above values for the global metal abundance, and our estimate of the cluster HB type we derive that the average mass of NGC 2419 RR

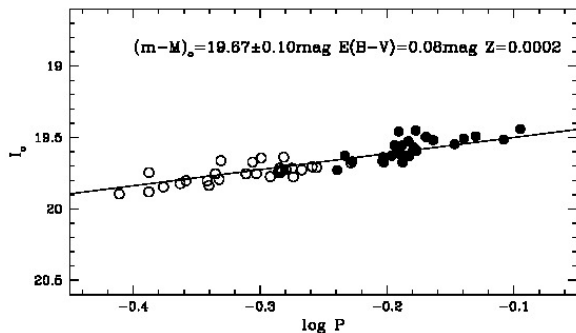


Fig. 12.— Comparison between predicted and observed RR Lyrae period-luminosity relation in the  $I$  band (symbols are as in Fig. 10). Periods of the c-type variables were fundamentalized by adding the value  $+0.127$  to the logarithm of the star period (see Di Criscienzo et al. 2004). The solid line shows the predicted relation for  $Z=0.0002$ .

Lyrae stars is in the range from  $0.74$  to  $0.69 M_{\odot}$ . Using instead the period ratio of the double-mode RR Lyrae star  $P_1/P_0=0.745$  and the Petersen diagram as suggested by Bragaglia et al. (2001) and Bono et al. (1996) we would derive a larger value of the mean mass of  $\sim 0.80 M_{\odot}$ . To take in account the uncertainty in the mass using a conservative approach we adopted a mass of  $M=0.72 M_{\odot}$  and varied this value by  $\pm 0.05 M_{\odot}$  when calculating quantities depending on mass.

### 5.2.1. FOBE and FRE

To apply this method we have first calculated the theoretical absolute visual magnitude of first-overtone blue edge and fundamental red edge, namely  $M_V(\text{FOBE})$  and  $M_V(\text{FRE})$ , by means of equations 2 and 3 in Di Criscienzo et al. (2004). These relations depend on the stellar mass and mixing length parameter  $l/H_p$ . For the mass value we used  $0.72 M_{\odot}$ , as discussed above, while for  $l/H_p$  we followed the prescriptions by Di Criscienzo et al. (2004), i.e  $l/H_p=1.5$  for the FOBE and  $l/H_p=2.0$  for the FRE. The results of this procedure are shown in Fig. 10. The distance modulus required to match the observed boundaries of the IS with the theoretical relations is  $(m-M)_0=19.63\pm 0.11$  mag, where the error takes into

account a variation of  $0.05 M_{\odot}$  in stellar mass, an error of  $0.04$  in the mixing length parameter, and the standard deviation of the relations ( $0.07$  dex).

### 5.2.2. Wesenheit function

This second method uses the predicted Wesenheit function in the  $V$  and  $I$  filters<sup>8</sup>. According to equation 4b in Di Criscienzo et al. (2004), to apply this relation we need three observed quantities, namely the mean  $V$  magnitude, the mean  $(V-I)$  color, and the period of each RR Lyrae star (once the mass is fixed at  $0.72 M_{\odot}$ ). The application of the method to the NGC 2419 RR Lyrae stars is shown in Fig. 11 where the c-type RR Lyrae stars were fundamentalized by adding  $+0.127$  to the logarithm of the first overtone period (see Di Criscienzo et al. 2004). The resulting distance modulus is  $(m-M)_0=19.70\pm 0.09$  mag, where again the error takes into account the error in mass, and the intrinsic dispersion of the adopted theoretical relation ( $\sim 0.03$  mag).

### 5.2.3. Period-Luminosity relation

The third method involves the use of the Period-Luminosity (PL) relation in the  $I$  band. This correlation is not as tight as the  $K$  band (PL), but is sufficiently well defined to be used as a reliable distance indicator. In this work we used the relationship given by Catelan et al. (2004), based on synthetic HB models, which essentially depends on the overall metallicity  $Z$ . The derived distance modulus adopting  $Z=0.0002$  is  $(m-M)_0=19.67 \pm 0.10$  mag where the error is mainly due to uncertainty on the adopted  $Z$ . We note that the value adopted for  $Z$  falls in the range derived in Section 5.2.

### 5.2.4. Light curve model fitting

Further constraints on the distance to NGC 2419 can be obtained by the model fitting of the observed light curves with nonlinear convective hydrodynamical models (see e.g. Di Criscienzo et al. 2004; Bono, Marconi & Stellingwerf 1999). This very promising technique was already applied

<sup>8</sup>We have chosen to use the  $V$  and  $I$  bands because the SUBARU data have higher quality compared to the TNG  $B$  data.

with success to field and cluster RR Lyrae stars by Bono et al. (2000); Marconi & Clementini (2005); Marconi & Degl’Innocenti (2007). In the case of the RR Lyrae stars in NGC 2419 we have well sampled light curves in at least one photometric band (the  $V$  band), allowing in principle to apply the method to an extensive and homogeneous sample of pulsators. For a preliminary application in this paper we have selected one fundamental mode RR Lyrae star, variable V3, and two first overtone RR Lyrae stars, V34 and V75.

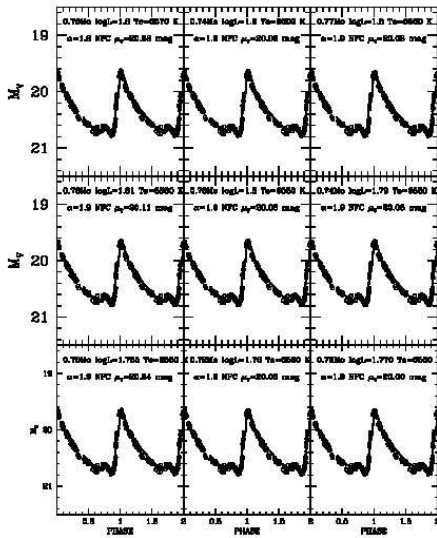


Fig. 13.— Results from the theoretical modeling of the observed  $V$ -band light curve for the RRab star V3. The best fit model parameters: effective temperature, mass and luminosity are labelled together with the adopted mixing length value and the inferred  $V$ -band apparent distance moduli, assuming  $E(B - V) = 0.08$  mag.

By using the procedure outlined in Marconi & Clementini (2005); Marconi & Degl’Innocenti (2007) and references therein, for the three pulsators we computed a set of pulsation models varying the stellar parameters in order to reproduce the period, the amplitude and the morphology of the observed light curves. In particular, we fixed the chemical composition ( $Z = 0.0002$ ,  $Y = 0.24^9$ ) and allowed

<sup>9</sup>We chose this value for the helium abundance as it is close

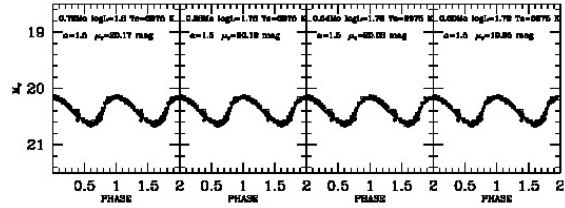


Fig. 14.— Same as figure Fig. 13 for the RRC star V34.

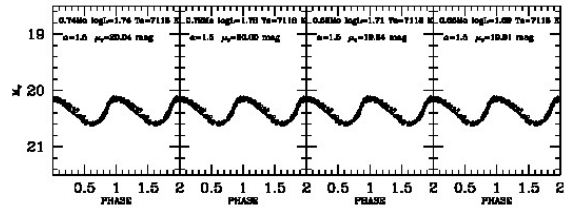


Fig. 15.— Same as figure Fig. 13 for the RRC star V75.

the mass (and, as a consequence, the luminosity at fixed effective temperature) to vary in the interval suggested by synthetic HB models (see the discussion on the mass given at the beginning of this section). As a result we defined the best effective temperature for which the pulsation models are able to reproduce the observed light variations within  $\pm 0.05$  mag over all the pulsation cycle for stellar masses and luminosities consistent with the evolutionary prescriptions. In Figs. 13, 14, and 15 we show the best fit solutions (solid lines) overimposed to the observed  $V$  band light curves. The inferred stellar parameters and distance moduli are labelled in each panel. In the case of V75 we find,  $\mu$  of  $\pm 0.07$  mag on the inferred apparent distance modulus of 19.73 mag. For V34 we find,  $\mu$  of  $\pm 0.11$  mag on the inferred apparent distance modulus of 19.83 mag, whereas for the RRab star V3 an uncertainty of  $\pm 0.04$  in mass causes an error of  $\pm 0.08$  mag on the derived distance modulus of 19.81 mag. The errors on the inferred distance moduli have to be increased to take into

to the Big Bang value (Coc et al. 2004).

account also the contribution of photometric and reddening uncertainties.

### 5.2.5. Summary of the distance estimates

Distances to NGC 2419 obtained by the various methods described above are summarized in Table 4: all these estimates are consistent to each other within their uncertainties. Although results from the model fitting tend to provide fainter distance moduli than the other methods. A mean of the values in Table 4 weighting each individual value by its error leads the mean distance modulus of  $\mu_0$  (NGC 2419) =  $19.714 \pm 0.078$  mag, while a simple mean would lead to  $\mu_0$  (NGC 2419) =  $19.717 \pm 0.078$  mag. A mean computed discarding the longest and shortest moduli would lead to  $\mu_0$

variable stars “fundamentalized” according to the method described by various authors in the literature (see e.g. McNamara, Clementini & Marconi 2007). Following these authors stars brighter than the PL relation in the period-magnitude plane are pulsating in a different pulsation mode. In particular, by adopting the slope of the PL relation by McNamara et al. (2004) the SX Phoenicis stars lying above the relation in the period-magnitude plane (Fig. 16) are first overtone (FO) pulsators. As  $P_{FO}/P_F=0.775$  (Poretti et al. 2005), these stars must be shifted rightwards by 0.111 dex in order to fundamentalize them (open circle in Fig. 16). Applying this shift all the stars seem to lie on the same well defined PL relation. Using the PL slope by McNamara et al. (2004), and  $E(B-V)=0.08$  we obtain  $\mu_0=19.72 \pm 0.10$  mag (see also Fig. 16) in good agreement with the distance values found with methods based on the RR Lyrae stars.

## 7. Conclusions

We have presented a new photometric study of the variable stars in the remote Galactic globular cluster NGC 2419, using proprietary and archive  $B, V, I$  time-series CCD photometry of the cluster which span a large time interval and cover a total area of  $50 \times 43$  arcmin<sup>2</sup> centered on NGC 2419 (see Paper I). Variable stars were identified using the image subtraction technique. We recovered and confirmed periods for all the variables previously known in the cluster (41 objects) by PR photographic study, as well as discovered 60 new variables, doubling the number of RR Lyrae stars. The new discoveries include 11 fundamental mode and 28 first overtone pulsators increases by a factor 5 the statistics of the RRc stars detected in NGC 2419 by PR. Most of the new RRc stars as well as the new RRab stars with longer periods were missed by PR because their small amplitudes and the location often towards the cluster center made them rather difficult to detect with traditional techniques and photographic data. In our study we also detected 12 cluster SX Phoenicis stars. In this paper we have presented the catalogue of light light curves for all the 101 variables of NGC 2419. and studied in detail their properties. Both RR Lyrae and SX Phe stars were used to estimate the cluster distance by means of a variety of different and in

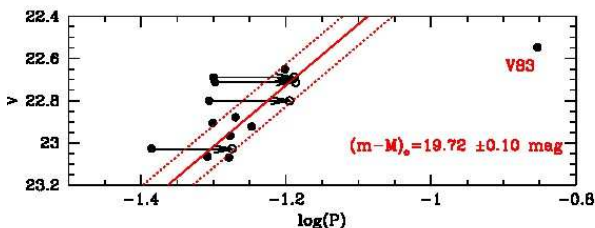


Fig. 16.— Position of the SX Phe stars in the  $V - \log P$  plane (filled circles). Open circles are variables “fundamentalized” according to the procedure described in the text. The solid line is the PL relation by McNamara et al. (2004) using the labelled value of distance modulus.

The mean apparent  $V$  magnitudes of the 12 SX Phoenicis stars discovered in NGC 2419 are plotted versus the observed periods (filled circle) in Fig. 16. In the figure open circles represent

same cases independent methods. The final distance modulus derived for NGC 2419 from its RR Lyrae population is:  $\mu_0$  (NGC 2419) =  $19.71 \pm 0.08$  mag corresponding to  $D = 87.5 \pm 3.3$  kpc, in good agreement with the modulus derived from the cluster SX Phe stars and results from other methods in the literature. The improved number of RR Lyrae stars and a detailed analysis of their pulsation properties were used to re-evaluate the Oosterhoff classification of NGC 2419 and get hints on the intriguing nature of this cluster. We confirm a “pure” OoII classification for NGC 2419 as also suggested by the cluster metallicity, this would disfavor an extragalactic origin for NGC 2419, since RR Lyrae stars in extragalactic systems (e.g. field and cluster RR Lyrae stars in the Magellanic Clouds and in classical dwarf spheroidal galaxies) generally have properties intermediate between OoI and II types (Catelan 2004, 2005). However, the OoII behaviour of NGC 2419, by itself, is not a sufficient condition to conclude that the origin of NGC 2419 is not extragalactic. Indeed, 5 of the LMC GCs and the Ursa Minor dSph also have OoII type. Moreover, most of the ultrafaint dwarf spheroidal galaxies recently discovered by the SDSS (e.g. Bootes I, Canes Venatici II, Coma, Leo IV, and UMa II) are found to be pure Oosterhoff type II systems (Cseresnyes 2001; Dall’Ora et al. 2006; Greco et al. 2008; Musella et al. 2008; Moretti et al. 2009).

In conclusion current results for NGC 2419 stellar content (including the variable stars) do not allow us to explain why this cluster is anomalous both as a globular cluster and as a possible remnant of a disrupted dwarf galaxy, pointing toward the need of a detailed analysis of the CMD and in particular of its HB.

Our data providing a first complete mapping of the cluster HB, from the extreme “blue hook” to the red portion, have opened the possibility for such a study through theoretical evolutionary models and synthetic populations. Such a study is under way and will be of great importance to put constraints of the origin of NGC 2419.

Financial support for this study was provided by PRIN MIUR 2007 (P.I: Piotto). M.D.C thanks the Osservatorio di Bologna for hospitality during her stay when part of this work was done and F. D’Antona for very interesting discussions on the

still mysterious nature of NGC 2419.

Table 1: Instrumental set-ups and logs of the observations.

| Dates                    | Telescope | Instrument  | Resolution            | FOV                     | $N_B$ | $N_V$ | $N_I$ | Photometric accuracy<br>(HB level) |
|--------------------------|-----------|-------------|-----------------------|-------------------------|-------|-------|-------|------------------------------------|
| UT                       |           |             | ( $''/\text{pixel}$ ) |                         |       |       |       | (mag)                              |
| Sept., 2003 - Feb., 2004 | TNG       | Dolores     | 0.275                 | $9.4' \times 9.4'$      | 20    | 22    | ...   | 0.01-0.03                          |
| May, 1994 - Mar., 2000   | HST       | WFPC2       | 0.1                   | $\sim 2.5' \times 2.5'$ | ...   | 18    | 10    | 0.1-0.15                           |
| Nov., 1997               | HST       | WFPC2       | 0.1                   | $\sim 2.5' \times 2.5'$ | ...   | 7     | 39    | 0.1-0.15                           |
| Dec., 2002               | SUBARU    | Suprime-Cam | 0.20                  | $34' \times 27'$        | ...   | 165   | 16    | 0.01-0.02                          |

Table 2:  $V, B, I$  time series photometry of the variable stars. A portion of Table 2 is shown here for guidance regarding its form and content. The entire catalog is available from the authors upon request.

| Star V3 - RRab              |            |                             |            |                             |            |
|-----------------------------|------------|-----------------------------|------------|-----------------------------|------------|
| HJD<br>(-2452609)<br>(days) | V<br>(mag) | HJD<br>(-2452905)<br>(days) | B<br>(mag) | HJD<br>(-2452609)<br>(days) | I<br>(mag) |
| 0.051979                    | 20.303     | 0.746271                    | 20.256     | 0.038409                    | 20.124     |
| 0.053994                    | 20.294     | 1.754012                    | 21.198     | 0.039415                    | 20.009     |
| 0.055001                    | 20.450     | 86.592255                   | 20.666     | 0.040420                    | 20.040     |
| 0.056019                    | 20.487     | 86.606125                   | 20.714     | 0.041426                    | 19.929     |
| 0.057028                    | 20.034     | 86.619461                   | 20.796     | 0.042435                    | 20.107     |
| 0.058034                    | 20.070     | 86.628792                   | 20.816     | 0.043442                    | 20.030     |
| 0.059041                    | 20.046     | 86.638573                   | 20.835     | 0.044447                    | 20.190     |
| 0.061506                    | 20.068     | 127.485786                  | 21.189     | 0.045453                    | 19.502     |

TABLE 3

IDENTIFICATION AND PROPERTIES OF NGC 2419 VARIABLE STARS. NOTES ON INDIVIDUAL STARS ARE PROVIDED IN SECTION 3.1.

| Name | Id      | RA(J2000)   | DEC(J2000)  | Type   | P         | Epoch       | $\langle V \rangle$ | $A_V$        | $\langle B \rangle$ | $A_B$        | $\langle I \rangle$ | $A_I$        |
|------|---------|-------------|-------------|--------|-----------|-------------|---------------------|--------------|---------------------|--------------|---------------------|--------------|
| V01  | 17997   | 7:38:11.611 | 38:51:58.95 | LPV    | 198.0     | 52617.00    | 17.437              | $\geq 0.477$ | 18.925              | $\geq 0.691$ | 16.116              | indef        |
| V02  | 23327   | 7:38:07.955 | 38:52:33.67 | RRab   | 0.670170  | 53030.5599  | 19.331              | 0.881        | 19.845              | $\geq 0.781$ | 18.481              | $\geq 0.232$ |
| V03  | 22280   | 7:38:12.705 | 38:52:27.36 | RRab   | 0.625986  | 52617.0987  | 20.344              | 1.091        | 20.755              | $\geq 1.101$ | 19.783              | $\geq 0.781$ |
| V04  | 23625   | 7:38:15.128 | 38:52:35.12 | RRc    | 0.39210   | 52609.1238  | 20.317              | 0.502        | 20.698              | 0.672        | 19.843              | indef        |
| V05  | 33749   | 7:38:11.142 | 38:53:38.78 | RRab   | 0.655868  | 52608.667   | 20.180              | $\geq 1.048$ | 20.591              | $\geq 1.334$ | 19.645              | indef        |
| V06  | 10150   | 7:38:12.889 | 38:50:43.78 | RRc    | 0.371609  | 52617.1148  | 20.373              | 0.596        | 20.749              | $\geq 0.638$ | 19.871              | $\geq 0.276$ |
| V07  | 39159   | 7:38:16.185 | 38:54:18.79 | RRab   | 0.627331  | 52611.095   | 20.357              | 1.088        | 20.822              | $\geq 0.766$ | 19.793              | $\geq 0.267$ |
| V08  | 33054   | 7:38:06.842 | 38:53:34.14 | LPV    | 13.0      | 52581.470   | 17.362              | 0.118        | 18.722              | 0.141        | 15.830              | indef        |
| V09  | 21821   | 7:38:05.633 | 38:54:21.16 | RRab   | 0.644733  | 52608.365   | 20.219              | $\geq 0.798$ | 20.671              | $\geq 0.556$ | indef               | indef        |
| V10  | 18271   | 7:38:09.890 | 38:52:01.07 | LPV    | 19.05     | 53053.400   | 17.123              | 0.344        | 18.542              | $\geq 0.419$ | 15.483              | indef        |
| V11  | 24835   | 7:38:16.425 | 38:52:42.26 | RRab   | 0.58918   | 52609.0141  | 20.339              | $\geq 0.779$ | 20.753              | $\geq 0.342$ | 19.809              | $\geq 0.438$ |
| V12  | 41437   | 7:38:19.788 | 38:54:40.96 | RRab   | 0.661875  | 52608.6917  | 20.268              | 0.970        | 20.724              | $\geq 0.850$ | 19.792              | indef        |
| V13  | 24488   | 7:38:16.926 | 38:52:40.20 | RRab   | 0.640267  | 52609.005   | 20.304              | 0.885        | 20.806              | $\geq 1.023$ | 19.676              | indef        |
| V14  | 24717   | 7:37:58.391 | 38:52:42.30 | RRab   | 0.741325  | 52610.0986  | 20.238              | 0.962        | 20.668              | $\geq 0.850$ | 19.610              | $\geq 0.176$ |
| V15  | 32575   | 7:38:13.662 | 38:53:30.62 | RRab   | 0.640006  | 52608.0384  | 20.283              | 0.858        | 20.790              | $\geq 0.579$ | 19.672              | indef        |
| V16  | 37246   | 7:38:12.380 | 38:54:03.39 | RRab   | 0.666080  | 53032.4811  | 20.295              | 1.124        | 20.669              | $\geq 1.25$  | 19.712              | indef        |
| V17  | 41439   | 7:38:17.740 | 38:54:40.95 | RRab   | 0.649043  | 52609.060   | 20.319              | 1.134        | 20.764              | $\geq 1.088$ | 19.687              | indef        |
| V18  | 41939   | 7:38:07.165 | 38:54:46.81 | Cep II | 1.578669  | 53032.481   | 18.873              | 0.750        | 19.414              | $\geq 0.907$ | 18.234              | $\geq 0.492$ |
| V19  | 20251   | 7:37:59.022 | 38:52:15.01 | RRab   | 0.70260   | 52611.1197  | 20.284              | 0.952        | 20.758              | $\geq 0.387$ | 19.735              | $\geq 0.532$ |
| V20  | 33657   | 7:38:05.958 | 38:53:38.19 | LPV    | 52.95     | 52650.0     | 17.386              | $\geq 0.278$ | 18.692              | $\geq 0.351$ | 15.925              | indef        |
| V21  | 31470   | 7:38:03.576 | 38:53:23.70 | RRab   | 0.686094  | 53032.5260  | 20.202              | 1.074        | 20.676              | $\geq 1.164$ | 19.637              | indef        |
| V22  | 25180   | 7:38:17.651 | 38:52:44.35 | RRab   | 0.576645  | 53032.4912  | 20.363              | 1.109        | 20.759              | $\geq 1.304$ | 19.847              | $\geq 0.392$ |
| V23  | 38186   | 7:38:10.696 | 38:54:10.73 | RRab   | 0.62650   | 52610.1163  | 20.368              | 1.029        | 20.792              | $\geq 1.200$ | 19.758              | $\geq 0.212$ |
| V24  | 25237   | 7:37:55.611 | 38:52:45.71 | RRab   | 0.652695  | 52617.1470  | 20.365              | 0.886        | 20.817              | $\geq 0.750$ | 19.747              | indef        |
| V25  | 32709   | 7:38:03.277 | 38:53:31.71 | RRab   | 0.636274  | 52608.450   | 20.334              | 1.076        | 20.864              | $\geq 0.800$ | 19.746              | $\geq 0.187$ |
| V26  | 7326    | 7:38:02.200 | 38:52:03.20 | RRab   | 0.66492   | 52610.0787  | 20.178              | 0.923        | 20.633              | 1.085        | 19.569              | indef        |
| V27  | 12101   | 7:38:09.776 | 38:51:09.04 | RRc    | 0.34519   | 53033.570   | 20.407              | $\geq 0.275$ | 20.782              | $\geq 0.235$ | 19.926              | indef        |
| V28  | 36163   | 7:37:51.813 | 38:53:56.14 | RRab   | 0.64560   | 52609.617   | 20.350              | $\geq 0.675$ | ...                 | ...          | 19.739              | $\geq 0.133$ |
| V29  | 25528   | 7:38:03.261 | 38:52:46.94 | RRab   | 0.725560  | 53032.4811  | 20.278              | 0.777        | 20.664              | $\geq 0.864$ | 19.626              | $\geq 0.175$ |
| V30  | 30275   | 7:38:06.094 | 38:53:16.18 | RRab   | 0.584618  | 53032.5910  | 20.322              | 1.065        | 20.513              | 1.343        | 19.745              | $\geq 0.419$ |
| V31  | 5001910 | 7:38:21.244 | 38:50:22.92 | RRc    | 0.38753   | 52608.89150 | 20.344              | 0.493        | 20.699              | 0.589        | 19.853              | $\geq 0.216$ |
| V32  | 34111   | 7:38:06.700 | 38:53:40.79 | RRab   | 0.64224   | 52608.3298  | 20.147              | $\geq 0.680$ | 20.610              | $\geq 0.830$ | 19.570              | indef        |
| V33  | 23396   | 7:38:12.269 | 38:52:33.92 | RRc    | 0.41117   | 52608.7635  | 20.323              | 0.474        | 20.685              | 0.535        | 19.824              | 0.09         |
| V34  | 44725   | 7:38:10.337 | 38:55:29.06 | RRc    | 0.403547  | 53053.5391  | 20.364              | 0.482        | 20.750              | 0.595        | 19.845              | indef        |
| V35  | 27712   | 7:38:12.009 | 38:52:59.86 | RRab   | 0.677207  | 53053.58012 | 20.265              | 0.867        | 20.695              | 1.097        | 19.614              | indef        |
| V36  | 33246   | 7:38:10.301 | 38:53:35.31 | RRab   | 0.64822   | 52991.6243  | 20.299              | 0.773        | 20.644              | $\geq 0.907$ | 19.676              | 0.227        |
| V37  | 29181   | 7:38:11.197 | 38:53:09.06 | RRab   | 0.6610265 | 52991.6340  | 20.276              | $\geq 1.056$ | 20.582              | 1.203        | 19.714              | indef        |
| V38  | 18676   | 7:38:08.132 | 38:52:03.94 | RRc    | 0.368980  | 52911.6340  | 20.248              | 0.457        | 20.583              | 0.571        | 19.791              | $\geq 0.286$ |
| V39  | 10671   | 7:38:10.715 | 38:50:51.10 | RRd    | 0.40703   | 52609.070   | 20.344              | 0.474        | 20.571              | $\geq 0.409$ | 19.909              | $\geq 0.265$ |
| V40  | 25629   | 7:38:13.089 | 38:52:47.21 | RRab   | 0.5756470 | 50770.1022  | 20.217              | 1.074        | 20.605              | 1.359        | 19.631              | 0.922        |
| V41  | 31405   | 7:38:07.200 | 38:53:23.10 | RRc    | 0.396460  | 53032.51155 | 20.334              | 0.430        | 20.751              | $\geq 0.560$ | 19.834              | 0.233        |
| V42  | 25357   | 7:38:08.719 | 38:52:45.74 | RRab   | 0.610078  | 52806.7635  | 20.293              | 0.758        | 20.036              | $\geq 0.882$ | 19.689              | $\geq 0.704$ |
| V43  | 23674   | 7:38:07.564 | 38:52:35.13 | RRc    | 0.379955  | 52610.154   | 20.222              | 0.147        | ...                 | ...          | 19.814              | indef        |
| V44  | 24629   | 7:38:09.672 | 38:52:41.32 | NC     | 0.87583   | 52906.7493  | 17.393              | 0.174        | 18.681              | 0.243        | 15.898              | indef        |
| V45  | 26853   | 7:38:06.530 | 38:52:54.84 | RRc    | 0.31394   | 52610.12    | 20.387              | 0.195        | 20.188              | $\geq 0.602$ | ...                 | ...          |
| V46  | 26160   | 7:38:06.448 | 38:52:50.76 | RRab   | 0.774047  | 50771.35    | 20.217              | $\geq 0.622$ | 20.454              | $\geq 0.442$ | 19.679              | $\geq 0.135$ |
| V47  | 15945   | 7:38:08.600 | 38:53:14.68 | RRab   | 0.65684   | 52617.0368  | 20.312              | $\geq 0.622$ | 20.540              | $\geq 0.296$ | 19.748              | indef        |
| V48  | 24628   | 7:38:10.035 | 38:52:41.15 | RRc    | 0.374897  | 50771.27149 | 20.214              | 0.476        | 20.367              | $\geq 0.493$ | 19.762              | $\geq 0.250$ |
| V49  | 30239   | 7:38:08.131 | 38:53:15.87 | RRc    | 0.327090  | 50771.23356 | 20.364              | 0.510        | 20.157              | $\geq 0.301$ | 19.959              | 0.361        |
| V50  | 16182   | 7:38:07.980 | 38:53:16.22 | RRab   | 0.698385  | 50770.68    | 20.191              | $\geq 0.653$ | 20.254              | $\geq 0.617$ | 19.522              | $\geq 0.358$ |
| V51  | 27292   | 7:38:06.188 | 38:52:57.50 | RRc    | 0.348446  | 49493.477   | 20.195              | 0.530        | ...                 | ...          | 19.781              | 0.342        |
| V52  | 29702   | 7:38:09.594 | 38:53:12.36 | RRc    | 0.332284  | 52609.0579  | 20.427              | 0.410        | 20.472              | $\geq 0.469$ | 19.856              | $\geq 0.273$ |
| V53  | 30464   | 7:38:07.782 | 38:53:17.29 | RRab   | 0.658467  | 50770.7191  | 20.007              | 0.805        | 20.347              | $\geq 0.889$ | ...                 | ...          |
| V54  | 13009   | 7:38:10.532 | 38:52:50.64 | RRc    | 0.43164   | 52609.11    | 19.410              | 0.260        | 19.622              | 0.146        | 18.860              | $\geq 0.081$ |
| V55  | 27613   | 7:38:05.994 | 38:52:59.62 | RRc    | 0.387675  | 53032.500   | 20.311              | 0.400        | 20.599              | 0.447        | 19.832              | $\geq 0.323$ |
| V56  | 21790   | 7:38:07.987 | 38:52:24.65 | RRc    | 0.305795  | 49495.320   | 20.286              | 0.287        | ...                 | ...          | 19.864              | indef        |
| V57  | 24846   | 7:38:06.004 | 38:52:42.72 | RRab   | 0.736379  | 51622.095   | 19.948              | 0.741        | 20.511              | $\geq 0.713$ | 19.316              | 0.575        |
| V58  | 27780   | 7:38:10.644 | 38:53:00.3  | RRc    | 0.388238  | 52617.060   | 20.340              | 0.472        | 20.560              | 0.546        | 19.863              | $\geq 0.290$ |
| V59  | 29251   | 7:38:10.426 | 38:53:09.50 | RRab   | 0.803492  | 53033.515   | 20.233              | 0.527        | 20.562              | 0.593        | 19.559              | $\geq 0.358$ |

Table 4: Distances to NGC 2419 obtained using different methods based on the cluster RR Lyrae stars.

| $(m-M)_0$<br>(mag) | error<br>(mag) | method         |
|--------------------|----------------|----------------|
| 19.65              | $\pm 0.09$     | $M_V - [Fe/H]$ |
| 19.63              | $\pm 0.11$     | FOBE           |
| 19.70              | $\pm 0.09$     | PW             |
| 19.67              | $\pm 0.10$     | PLI            |
| 19.83              | $\pm 0.11$     | FIT-V34        |
| 19.73              | $\pm 0.07$     | FIT-V75        |
| 19.81              | $\pm 0.08$     | FIT-V3         |

## REFERENCES

- Alard C., 1999, A&A, 343, 10
- Alard, C., 2000, A&AS, 144, 363
- Baade, W., 1935, ApJ, 82, 396B
- Baumgardt, H., Coté, P., Hilker, M., Rejkuba, M., Mieske, S., Djorgovski, S. G., Stetson, P. 2009, MNRAS, 396, 2051
- Bedin, C., Piotto, G., Anderson, J., Cassisi, S., King, I., Momany, Y., Carraro, G., 2004, A&AS, 605, 125
- Barning, F. J. M., 1963, Bull. Astron. Inst. Netherlands, 17, 22
- Bellazzini, M., 2004a, MNRAS, 347, 119
- Bellazzini, M., 2007, A&A, 473, 171
- Bellazzini, M., Ibata, R. A., Chapman, S. C., Mackey, A. D., Monaco, L., Irwin, M. J., Martin, N. F., Lewis, G. F., & Dalessandro, E. 2008, AJ, 136, 1147
- Blazhko, S. 1907, Astron. Nachr., 175, 325
- Bono, G., Caputo, F., Castellani, V., & Marconi, M. 1997 A&AS, 121, 327
- Bono, G., Caputo, F., Castellani, V. & Marconi, M., ApJ, 471, 33B
- Bono, G., Castellani, V. & Marconi, M., ApJ, 532, 129
- Bragaglia, A., Gratton, R. G., Carretta, E., Clementini, G., Di Fabrizio, L. & Marconi, M., 2001, AJ, 122, 207-219
- Brown, T. M., Sweigart, A. V., Lanz, T., Smith, E., Landsman, W. B., Hubeny, I. 2010, ApJ, 718, 1332
- Cacciari, C., & Clementini, G. 2003, in Stellar Candles for the Extragalactic Distance Scale, ed. D. Alloin and W. Gieren (Berlin: Springer, LNP), Lecture Notes in Physics, 635, 105
- Cacciari, C., Corwin, T. M., & Carney, B. 2005, AJ, 129, 267
- Caputo, F. 1997, MNRAS, 284, 994
- Caputo, F., Castellani, V., Marconi, M., Ripepi, V. 2000, MNRAS, 316, 819
- Carretta, E., Bragaglia, A., Gratton, R., D’Orazi, V. & Lucatello, S. 2009, A&A, accepted (arXiv0910.0675C)
- Catelan, M. 2004, ASP Conf. Ser. 310, 113
- Catelan, M., Pritzl, B. J., & Smith, H. A. 2004, ApJS, 154, 633C
- Catelan, M. 2005, (astro-ph/0507464)
- Christian, C. A., & Heasley, J. N., 1988, AJ, 95, 1422
- Clement, C. M., Nemec, J. 1990, AJ, 99, 240
- Clement, C. M., & Rowe, J. F 2000, AJ, 120, 2579
- Clementini, G., et al. 2000, AJ, 120, 2054
- Coc, A., Vangioni-Flam, E., Descouvemont, P., Adahchour, A., & Angulo, C. 2004, ApJ, 600, 544
- Corwin, T. M., et al. 2008, AJ, 135, 1459
- Clementini, G., Gratton, R., Bragaglia, A., Carretta, E., Di Fabrizio, L. & Maio, M. 2003, AJ, 125, 1309
- Cseresnjes, P. 2001, A&A, 375, 909
- Dall’Ora, M., et al. 2006, ApJ, 653, L109
- Dalessandro, E., Lanzoni, B., Ferraro, F. R., Vespe, F., Bellazzini, M., & Rood, R. T. 2008, ApJ, 681, 311

TABLE 3—Continued

| Name | Id      | RA(J2000)   | DEC(J2000)  | Type           | P         | Epoch       | $\langle V \rangle$ | $A_V$ | $\langle B \rangle$ | $A_B$        | $\langle I \rangle$ | $A_I$        |
|------|---------|-------------|-------------|----------------|-----------|-------------|---------------------|-------|---------------------|--------------|---------------------|--------------|
| V60  | 30716   | 7:38:06.659 | 38:53:18.83 | RRc            | 0.390496  | 52991.640   | 20.299              | 0.509 | 20.577              | 0.523        | 19.756              | $\geq 0.242$ |
| V61  | 8720    | 7:38:08.588 | 38:52:16.08 | SX Phe         | 0.05265   | 52608.9791  | 23.069              | 0.713 | 22.107              | indef        | 22.655              | indef        |
| V62  | 17882   | 7:38:08.324 | 38:53:31.44 | RRab           | 0.592503  | 52609.272   | 20.328              | 1.025 | 20.398              | $\geq 1.104$ | 19.786              | $\geq 0.549$ |
| V63  | 30364   | 7:38:10.979 | 38:53:16.44 | RRc            | 0.344915  | 52991.614   | 20.306              | 0.519 | 20.592              | 0.595        | 19.872              | 0.350        |
| V64  | 20512   | 7:38:10.293 | 38:52:16.34 | RRab           | 0.780009  | 49494.54495 | 20.314              | 0.456 | 20.526              | $\geq 0.419$ | 19.633              | indef        |
| V65  | 22441   | 7:38:11.321 | 38:52:28.18 | RRc            | 0.32278   | 52610.1154  | 20.109              | 0.230 | 20.691              | 0.341        | 19.453              | indef        |
| V66  | 29417   | 7:38:11.600 | 38:53:10.46 | RRc            | 0.386754  | 52611.143   | 20.340              | 0.443 | 20.523              | 0.593        | 19.863              | $\geq 0.261$ |
| V67  | 31497   | 7:38:10.970 | 38:53:23.47 | RRc            | 0.33989   | 52905.7417  | 20.364              | 0.453 | 20.672              | 0.557        | 19.922              | indef        |
| V68  | 25927   | 7:38:12.147 | 38:52:48.97 | RRc            | 0.364675  | 50768.5526  | 20.335              | 0.499 | 20.744              | 0.6          | 19.872              | 0.315        |
| V69  | 33596   | 7:38:10.641 | 38:53:37.73 | RRc            | 0.340932  | 53053.604   | 20.430              | 0.500 | 20.927              | $\geq 0.306$ | 19.954              | $\geq 0.062$ |
| V70  | 19518   | 7:38:08.468 | 38:53:46.63 | RRc            | 0.4155    | 52991.62    | 20.143              | 0.339 | 20.741              | 0.432        | 19.329              | $\geq 0.346$ |
| V71  | 17581   | 7:38:07.334 | 38:51:56.28 | SX Phe         | 0.049197  | 52608.976   | 23.066              | 0.418 | 23.459              | indef        | 22.730              | $\geq 0.166$ |
| V72  | 19747   | 7:38:09.923 | 38:53:49.52 | RRc            | 0.414626  | 52991.63404 | 20.376              | 0.455 | 20.772              | 0.577        | 19.828              | $\geq 0.088$ |
| V73  | 18388   | 7:38:11.521 | 38:52:01.76 | SX Phe         | 0.0528674 | 53053.57076 | 22.967              | 0.383 | 23.280              | $\geq 0.325$ | 22.505              | indef        |
| V74  | 25759   | 7:38:13.777 | 38:52:47.94 | RRc            | 0.305679  | 50771.07686 | 20.414              | 0.200 | 20.723              | 0.225        | ...                 | ...          |
| V75  | 20587   | 7:38:03.540 | 38:52:16.88 | RRc            | 0.3236    | 52991.6243  | 20.352              | 0.443 | 20.672              | 0.570        | 19.941              | $\geq 0.228$ |
| V76  | 18026   | 7:38:12.110 | 38:51:59.23 | RRc            | 0.44105   | 52608.650   | 20.301              | 0.474 | 20.544              | 0.531        | 19.795              | 0.278        |
| V77  | 19320   | 7:38:13.139 | 38:52:08.23 | RRc            | 0.38113   | 53032.4930  | 20.379              | 0.489 | 20.750              | $\geq 0.526$ | 19.892              | $\geq 0.151$ |
| V78  | 31821   | 7:38:13.752 | 38:53:25.53 | SX Phe         | 0.0411654 | 52905.7415  | 23.027              | 0.273 | 23.394              | $\geq 0.287$ | 22.690              | $\geq 0.142$ |
| V79  | 18137   | 7:38:13.194 | 38:52:00.02 | SX Phe         | 0.049438  | 52610.058   | 22.801              | 0.767 | 22.846              | 0.739        | 22.443              | $\geq 0.453$ |
| V80  | 16192   | 7:38:01.810 | 38:53:16.64 | RRab           | 0.6161    | 53053.595   | 20.648              | 0.604 | 21.336              | $\geq 0.838$ | ...                 | ...          |
| V81  | 36489   | 7:38:12.102 | 38:53:57.42 | SX Phe         | 0.0628808 | 53053.5807  | 22.651              | 0.424 | 22.975              | $\geq 0.471$ | 22.107              | indef        |
| V82  | 33557   | 7:38:13.847 | 38:53:37.34 | RRc            | 0.34728   | 53053.58012 | 20.318              | 0.303 | 20.658              | 0.376        | 19.912              | $\geq 0.155$ |
| V83  | 14335   | 7:38:08.535 | 38:51:31.40 | SX Phe(?)      | 0.14033   | 52608.5445  | 22.548              | 0.199 | 22.846              | 0.075        | 22.183              | indef        |
| V84  | 29591   | 7:38:01.459 | 38:53:11.99 | RRc            | 0.3271    | 52609.052   | 20.323              | 0.416 | 20.722              | $\geq 0.225$ | 19.921              | $\geq 0.163$ |
| V85  | 38108   | 7:38:01.849 | 38:54:10.44 | SX Phe         | 0.0499945 | 52608.97575 | 22.906              | 0.413 | 23.313              | $\geq 0.498$ | 22.587              | $\geq 0.218$ |
| V86  | 30259   | 7:38:19.618 | 38:53:15.74 | LPV            | 49.6      | 53053.591   | 17.466              | 0.289 | 18.825              | 0.437        | 15.919              | indef        |
| V87  | 13811   | 7:38:18.402 | 38:51:26.32 | Bin            | 0.233955  | 52617.14485 | 23.157              | 1.200 | 23.540              | 0.263        | 22.726              | 0.536        |
| V88  | 7517    | 7:38:10.573 | 38:49:53.37 | SX Phe         | 0.05372   | 52611.1386  | 22.879              | 0.281 | 23.126              | $\geq 0.193$ | 22.473              | 0.168        |
| V89  | 43459   | 7:38:19.777 | 38:55:07.35 | RRc            | 0.28972   | 52608.8022  | 20.409              | 0.079 | 20.701              | 0.064        | 20.014              | indef        |
| V90  | 5009772 | 7:38:23.136 | 38:54:11.64 | RRc            | 0.39742   | 52608.71826 | 20.392              | 0.457 | 20.765              | $\geq 0.490$ | 19.894              | indef        |
| V91  | 38530   | 7:37:52.824 | 38:54:14.42 | RRc            | 0.3893    | 52609.990   | 20.379              | 0.475 | ...                 | ...          | 19.846              | indef        |
| V92  | 347     | 7:38:51.641 | 38:53:49.61 | NC             | 5.63      | 52608.22    | 19.548              | 0.112 | ...                 | ...          | 18.162              | indef        |
| V93  | 2265    | 7:37:49.886 | 38:44:59.89 | SX Phe         | 0.05659   | 52608.5583  | 22.923              | 0.216 | ...                 | ...          | 22.463              | $\geq 0.100$ |
| V94  | 5015266 | 7:38:26.106 | 38:58:10.17 | RRab           | 0.71332   | 52610.050   | 20.318              | 0.590 | ...                 | ...          | 19.659              | indef        |
| V95  | 3462    | 7:37:29.362 | 38:54:33.92 | $\delta$ Scuti | 0.1483    | 52608.8198  | 19.228              | 0.064 | ...                 | ...          | 18.441              | 0.070        |
| V96  | 2513    | 7:37:39.605 | 38:51:35.81 | Bin            | 0.3597    | 52608.912   | 19.085              | 0.887 | ...                 | ...          | 17.629              | indef        |
| V97  | 3255    | 7:38:18.406 | 38:49:51.32 | SX Phe         | 0.05017   | 52608.9515  | 22.690              | 0.327 | ...                 | ...          | 22.341              | $\geq 0.162$ |
| V98  | 2254    | 7:37:38.956 | 38:50:22.02 | NC             | 0.2296    | 52610.0866  | 22.553              | 0.604 | ...                 | ...          | 20.221              | 0.285        |
| V99  | 5001168 | 7:38:28.628 | 38:49:15.4  | Bin            | 0.2015    | 526609.633  | 18.526              | 0.127 | ...                 | ...          | 16.461              | indef        |
| V100 | 4804    | 7:37:52.712 | 38:48:11.55 | $\delta$ Scuti | 0.13090   | 52608.940   | 18.335              | 0.264 | ...                 | ...          | 17.423              | indef        |
| V101 | 3528    | 7:38:14.881 | 38:50:24.74 | SX Phe         | 0.05038   | 52608.995   | 22.714              | 0.459 | ...                 | ...          | 22.080              | indef        |

- de Grijs, R., Wilkinson, M. I., & Tadhunter, C. N. 2005, MNRAS, 361, 311
- Di Criscienzo, M., Caputo, F., & Marconi, M. 2004, ApJ, 612, 1092
- D’Cruz, N. L., et al. 2000, ApJ, 530, 352
- Di Fabrizio, L. 1999, M.S. Thesis, Università degli studi di Bologna
- Eggen, O. J., Lynden-Bell, D., & Sandage, A. R. 1962, ApJ, 136, 748
- Faber, S. M., & Jackson, R. E. 1976, ApJ, 204, 668
- Gratton, R. G. and Bragaglia, A. and Clementini, G. & Carretta, E. and Di Fabrizio, L. and Maio, M. and Taribello, E. 2004., A&A, 421, 937-952
- Gratton, R., Sneden, C., & Carretta, E. 2004, ARA&A, 42, 385
- Greco, C. et al., 2008, ApJ, 675, 73
- Harris, W. E. 1996, AJ, 112, 1487
- Harris, W. E., et al. 1997, AJ, 114, 1030
- Johnson J. A. & Bolte, M. 1998, ApJ, 115, 693
- Kopacki, G. 2001, A&A, 369, 862
- Layden, A. C., & Sarajedini A. 2000, AJ, 119, 1760
- Lomb, N. R. 1976, Ap&SS, 39, 447
- McNamara, D. H., Rose, M. B., Brown, P. J., Ketcheson, D. I., Maxwell, J. E., Smith, K. M., & Wodey, R. C. 2004, in ASP Conf. Ser. 310, Variable Stars in the Local Group, ed. D. W. Kurtz & K. R. Pollard (San Francisco: ASP), 52
- Mackey, A. D., & Gilmore, G. F. 2004, MNRAS, 355, 504
- Mackey, A. D., & van den Bergh, S. 2005, MNRAS, 360, 631
- Marconi, M., & Clementini, G. 2005, MNRAS, 3129, 5527
- Marconi, M., & Degl’Innocenti, G. 2007, 2008, MmSAI, 79, 726M
- Momany, Y., Held, E.V., Saviane, I., Zaggia S., Rizzi, L., & Gullieuszik, M. 2007, A&A, 468, 973
- Monaco, L., et al., 2005, A&A, 441, 141
- Moretti, M.I., et al., 2009, ApJ, 699, 125
- Musella, I. et al. 2008, ApJ, 2008, 695, 83
- Newberg, H. J., et al. 2003, ApJ, 596, L191
- Norris, J. E. 2004, ApJ, 612, L25
- Oosterhoff, P. T. 1939, Bull. Astron. Inst. Netherlands, 9, 11
- Pinto, G., & Rosino, L. 1978, A&A, 28, 427
- Racine, R. & Harris, W. E. 1975, ApJ, 196, 413
- Reid, N. 1996, MNRAS, 278, 367
- Rey, S.-C., Lee, Y.-W., Ree, C. H., Joo, J.-M., Sohn, Y.-J., & Walker, A. R. 2004, AJ, 127, 958
- Ripepi, V., et al. 2007, ApJ, 667, 61
- Rosenberg, A., Aparicio, A., Saviane, I., Piotto, G. 2000, A&AS, 145, 451
- Rosenberg, A., Recio-Blanco, A., & García-Marín, M. 2004, ApJ, 603, 135
- Saha, A., Dolphin, A. E., Thim, F., & Whitmore, B. 2005, PASP, 117, 37
- Sandquist, E. L. & Hess, J. M. 2008, arXiv:0809.1782
- Scargle, J. D. 1982, ApJ, 263, 835
- Schlegel, D. J., Finkbeiner, & D. P., & Davis, M. 1998, ApJ, 500, 525
- Schwarzenberg-Czerny, A. 1996, ApJ, 460, L107
- Searle, L., & Zinn, R. 1978, ApJ, 225, 357
- Sirianni, M., et al. 2005, PASP, 117, 1049
- Sollima, A., Pancino, E., Ferraro, F. R., Bellazzini, M., Straniero, O., & Pasquini, L. 2005, ApJ, 634, 332
- Stetson, P. B. 1987, PASP, 99, 191
- Stetson, P. B. 1998, PASP, 110, 1448

- Stetson, P. B. 1992, in Worrall D. M., Biemesderfer C., Barnes J., eds, ASP Conf. Ser. 25, 297
- Stetson, P. B. 2005, PASP, 117, 563
- Suntzeff, N. B., Kraft, R. P., & Kinman, T. D. 1988, AJ, 95, 91
- Trager, S. C., King, I. R. & Djorgovski, S. 1995, AJ, 109, 218
- Walker, A. R. 1994, AJ, 108, 555
- Whitney, J. H., et al. 1998, ApJ, 495, 284
- van den Bergh, S., & Mackey, A. D. 2004, MNRAS, 354, 713
- Villanova, S., et al. 2007, ApJ, 663, 296
- Walker, S., 1998, AJ, 116, 230
- Zinn, R. 1993a, in Smith G. H., Brodie J. P., eds, ASP Conf. Ser. 48: The Globular Cluster-Galaxy Connection The Galactic Halo Cluster Systems: Evidence for Accretion.
- Zinn, R., & West, M. J. 1984, ApJS, 55, 45

